THE UNIVERSITY OF ALBERTA

A THREE DIMENSIONAL PHOTOELASTIC INVESTIGATION OF STRESS CONCENTRATIONS IN OPERABLY DEFORMED HUMAN TEETH.

A THESIS

SUBMITTED TO THE FACULTY OF GRADUATE STUDIES IN PARTIAL FULFILMENT OF THE REQUIREMENTS FOR THE DEGREE OF MASTER OF SCIENCE.

DEPARTMENT OF MECHANICAL ENGINEERING

by

Eric William Johnson, B.Sc. (Eng.)

Edmonton, Alberta

June, 1965.

UNIVERSITY OF ALBERTA

Faculty of Graduate Studies

The undersigned certify that they have read, and recommend to the Faculty of Graduate Studies for acceptance, a thesis entitled "A Three Dimensional Photoelastic Investigation of Operably Deformed Human Teeth" submitted by Eric William Johnson in partial fulfilment of the requirements for the degree of Master of Science.

ABSTRACT

A method is described for the manufacture and preparation of models of the first mandibular molar in 'HYSOL' epoxy resin. The models are modified to represent a variety of preparation shapes, comparable to those used in dental operations on human teeth. The models are then heated under load and cooled to "freeze" in the resulting stress pattern.

Although an absolute value of stress is not obtained, different shapes are compared for stress concentration.

ACKNOWLEDGMENTS

The author thanks Professors C. Castaldi, G. Ford, J.S. Kennedy and Dr. G.B. Davidson, for all their assistance and encouragement given in the preparation of this thesis.

Thanks are also due to the Department of Pediatric Dentistry for assistance with models and technical information and to the Department of Mechanical Engineering for considerable assistance in the manufacture of much of the equipment used in this investigation.

Finally, grateful thanks are given to Mr. Daniel Gau of the Department of Dentistry for very considerable assistance in the monotonous work of slice preparation.

E.W.J.

TABLE OF CONTENTS

Chapter		Page
-	Notation	1
-	Glossary	2
1	Introduction	6
2	Elementary Theory of Elasticity	9
	Two Dimensional Systems	9
	Three Dimensional Systems	13
3	Elementary Theory of Photoelasticity	14
	Plane Polarization	15
	Circular Polarization	23
4	Apparatus	37
5	Experimental Procedure	44
6	Results	48
7	Conclusions	69
8	Recommendations	70
-	Bibliography	71

Appendices

A	Detailed Procedure for Production of Models	73
B	Design Drawings for Polariscope	Folder 1
C	Design Drawings for Loading Frame	Folder 2
D	Additional Photographs of Stress Patterns in sections.	Folder 3

TABLE OF FIGURES

FIGURE	TITLE	PAGE
I	Two Dimensional Stress System acting on element of plane lamina.	10
II	MOHRS Circle, illustrating relation between normal and shear stresses acting on element of plane lamina.	12
III	Plane Polarized ray passing through loaded photoelastic model.	17
IV	Plane Polarized ray striking analyzer, after passing through loaded model.	20
V	Plane Polarized ray approaching Quarter Wave Plate.	25
VI	Circular Polarized ray approaching a loaded model.	26
VII	Diagrammatic arrangement of Transmission Polariscope.	31
VIII	Clamp for holding model slices in Polariscope.	36
IX	Polariscope adjusted to take photograph of section, using circular polarized light.	38
X	Model and loading frame for stress freezing.	41
XI	Closeup of model tooth under load.	41
XII	High reduction gearbox for oven thermostat control.	42
XIII	Scale drawing of Class I cavity.	45
XIV	Selection of model tooth slices.	57
XV	Selection of model tooth slices.	58
XVI	Comparison of stress patterns in models with artificial and natural pulp chambers.	59

XVII	Comparison of stress patterms in central sections of models having a variety of cavities.	61
XVIII	Comparison of stress patterns in mesial sections of models having a variety of cavities.	63
XIX	Comparison of stress patterns in distal sections of models having a variety of cavities.	65
XX	Mould, showing models as cast and after polishing.	78
XXI	Shaping model cavities on Unimat lathe.	80
XXII	Detail of machining model cavity.	81
XXIII	Polishing model slice on Trimmer.	83
XXIV	Final polishing of model slice.	85
XXV	Stress freezing in progress.	89

NOTATION

SYMBOLS USED

a	amplitude of incident beam of light in polariscope.
b	$\frac{a}{\sqrt{2}}$
C	stress optical coefficient for plastic used to make model.
f	frequence of incident light in polariscope.
s	transverse displacement of beam of light, after polarization, at time t.
t	time.
w	thickness of model.
α	angle between plane of polarization of light beam and axis of principal stress in model.
β	an arbitary angle between some reference plane and the plane of polarization of a light beam emerging from polarizer.
δ	angle between axis of principal stress in model, and axis of polarization of incident circularly polarized light.
Δ	phase difference between transmitted components of a beam of polarized light passing through a loaded model.
θ	angle between normal to any plane in model and x axis (used to define a plane on which stresses are acting).
λ	wavelength of incident light.
σ	normal stress
σ_x, σ_y, σ_z	principal stresses in three mutually perpendi-

cular directions acting at a point in the model.

τ shear stress

ψ ($2\pi ft$ + constant). The 'constant' depends on the refractive properties of the material being traversed by light beam and thus varies from plane to plane.

GLOSSARY

ANALYZER - a sheet of polarizing material used to examine the emergent ray from a birefringent model.

BIREFRINGENCY - a property of certain transparent materials. The velocity of light through material is not constant but varies directionally with the stress applied to the model.

BUCCOLINGUAL SECTION - a 'radial' section through tooth from cheek to tongue.

CIRCULAR POLARIZED LIGHT - beam of polarized light in which the tip of the vector representing the wave motion moves in a helix along the axis of the beam.

CROSSED POLARISCOPE - the planes of polarization of polarizer and analyzer are placed at 90°, so that no light is transmitted through them.

FRINGES - black lines seen in the field of a polariscope when monochromatic light is used to illuminate a loaded model, or coloured lines seen when white light is used.

FROZEN STRESSES - technique used to analyze three dimensional stress systems. A plastic model is heated

above a critical temperature and then cooled under continuous loading. A molecular change of state in the plastic at this critical temperature causes the fringe pattern to be "frozen" into model and this remains when load is removed.

ISOCHROMATICS - a family of fringes. Along these fringes the difference of the principal stresses, $(\sigma_x - \sigma_y)$ remains constant.

ISOCLINICS - a family of fringes. Along these fringes the inclination of the principal stresses (σ_x, σ_y), to some arbitary reference, remains constant.

MESIODISTAL SECTION - a section through tooth from front to rear, perpendicular to bucco-lingual section.

OCCLUSAL SURFACE - the biting surface of a tooth.

PLANE POLARIZED LIGHT - a beam of polarized light in which the plane of polarization has a constant inclination to an arbitary reference plane.

POLARIZER - a sheet of polarizing material used to convert a beam of ordinary light to plane polarized light.

PREPARATION - a cavity cut into a tooth to remove decayed material and provide a foundation for an

artificial filling.

PRINCIPAL DIRECTIONS - three mutually perpendicular directions at a point in a three dimensional stress system. No shear stresses act on planes perpendicular to these directions.

PRINCIPAL STRESSES - normal stresses acting in the principal directions.

QUARTER WAVE PLATES - sheets of polarizing material which provide a retardation of one quarter wave. Such a plate generates circularly polarized light and two in sequence are used to suppress isoclinics.

RESIDUAL STRESS - stress system found in plastic models before loading due to local deformation during manufacture.

STRESS CONCENTRATION - area in a loaded model in which stresses are appreciably higher than the average or in adjacent areas. Their presence is indicated in polariscope by a crowding together of the isochromatics.

Chapter 1

INTRODUCTION

For many years the problem of decay on human teeth has been studied.[1] A great amount of apparatus has been developed to simplify the operation necessary to halt or remove decay and to restore the tooth to its original profile, so that it may carry out its intended function.

Despite all these developments, restorations in teeth still fail,[2,3] either by the filling working loose and permitting further decay, or by the tooth itself fracturing. This undoes the previous operation and renders necessary a more complex restoration. Such repetition is tedious, sometimes painful to the patient, is costly and often inefficient.

Little attempt has been made, until recently, to 'design' cavities to conform to the known principles of good practice in the reduction of local stress concentrations. The cavity shapes currently used depend largely on clinical experience and empiricism. Models of teeth have been used extensively for many years to guide the dentist in his operations but little or no quantitative testing of tooth strength has been undertaken. This is due to the complicated shape, which defies mathematical analysis, and to the difficulty of identifying the points of highest stress concentration.

The development of photoelasticity and the more wide-

spread knowledge of its use[4] has introduced a new method of analysis. Within the last fifteen years, it has been used in an attempt to derive a more scientific basis for cavity design.[5,6,7,8,9] In all these investigations laminar models of a section or sections of teeth were prepared from sheet plastic, with birefringent properties.

The models were then loaded two-dimensionally and the locations of stress concentration observed in a polariscope. While this method provides some information, and has the merit of simplicity, the loading pattern used can bear little resemblance to that in the actual tooth. A tooth is normally loaded by contact with the matching teeth[10] and such contact takes place at many different points on the occlusal surface. The contact forces vary in intensity and direction and form a three dimensional force system.

Each of these loads contributes to the overall stress pattern in the tooth, which, it must be remembered, is quite small, rarely exceeding 10 mm. diameter.[11] Thus, a two-dimensional loading of a tooth section may ignore appreciable effects of adjacent loadings. In fact, in the investigation described below, significant stress concentrations have been observed in sections which contained no loading.

It was therefore decided to attempt to extend the scope of this previous work by use of three dimensional photoelastic analysis. The experimental work described

below had the following main objectives:-

(1) to establish a reliable and repeatable technique for the manufacture of plastic models of teeth free of residual stress.

(2) to establish techniques for the modification of these castings to represent filling cavities, and for loading these models, in a manner reasonably close to that found in real life, in such a way that the resultant stresses could be 'frozen' for subsequent examination.

(3) to demonstrate that localised modification of the shape of the cavity can reduce the maximum level of stress concentration and thus extend the life of the tooth.

Chapter 2

ELEMENTARY THEORY OF ELASTICITY

A short review follows of the theory of the distribution of stress in a loaded structure. This forms a foundation for the photoelastic theory in Chapter 3.

Two Dimensional Stress Systems

The distribution of stress in a component loaded in two dimensions may be analyzed by considering a small element of a uniform lamina of uniform unit thickness. The small element is subjected to normal stresses, $\sigma_{x'}$ and $\sigma_{y'}$, and shear stress $\tau_{x'y'}$. See Figure I.

Consider a plane MM through the Z axis at an angle θ' to the Y' axis (the normal to the plane makes an angle θ' with X' axis). If σ be the normal stress and τ the shear stress acting on the face BC of a small triangular element of the lamina, ABC, then, for equilibrium of this element

(a) in the X' direction: -

$$-AC\sigma_{x'} - AB\tau_{x'y'} + BC\sigma \cos\theta' - BC\tau \sin\theta' = 0 \tag{1}$$

(b) in the Y' direction:-

$$AB\sigma_{y'} + AC\tau_{x'y'} - BC\sigma \sin\theta' - BC\tau \cos\theta' = 0 \tag{2}$$

These equations yield;-

$$\sigma = \sigma_{x'} \cos^2\theta' + \sigma_{y'} \sin^2\theta' + \tau_{x'y'} \sin 2\theta' \tag{3}$$

$$\tau = (\sigma_{y'} - \sigma_{x'}) \sin\theta' \cos\theta' + \tau_{x'y'}(\cos^2\theta' - \sin^2\theta') \tag{4}$$

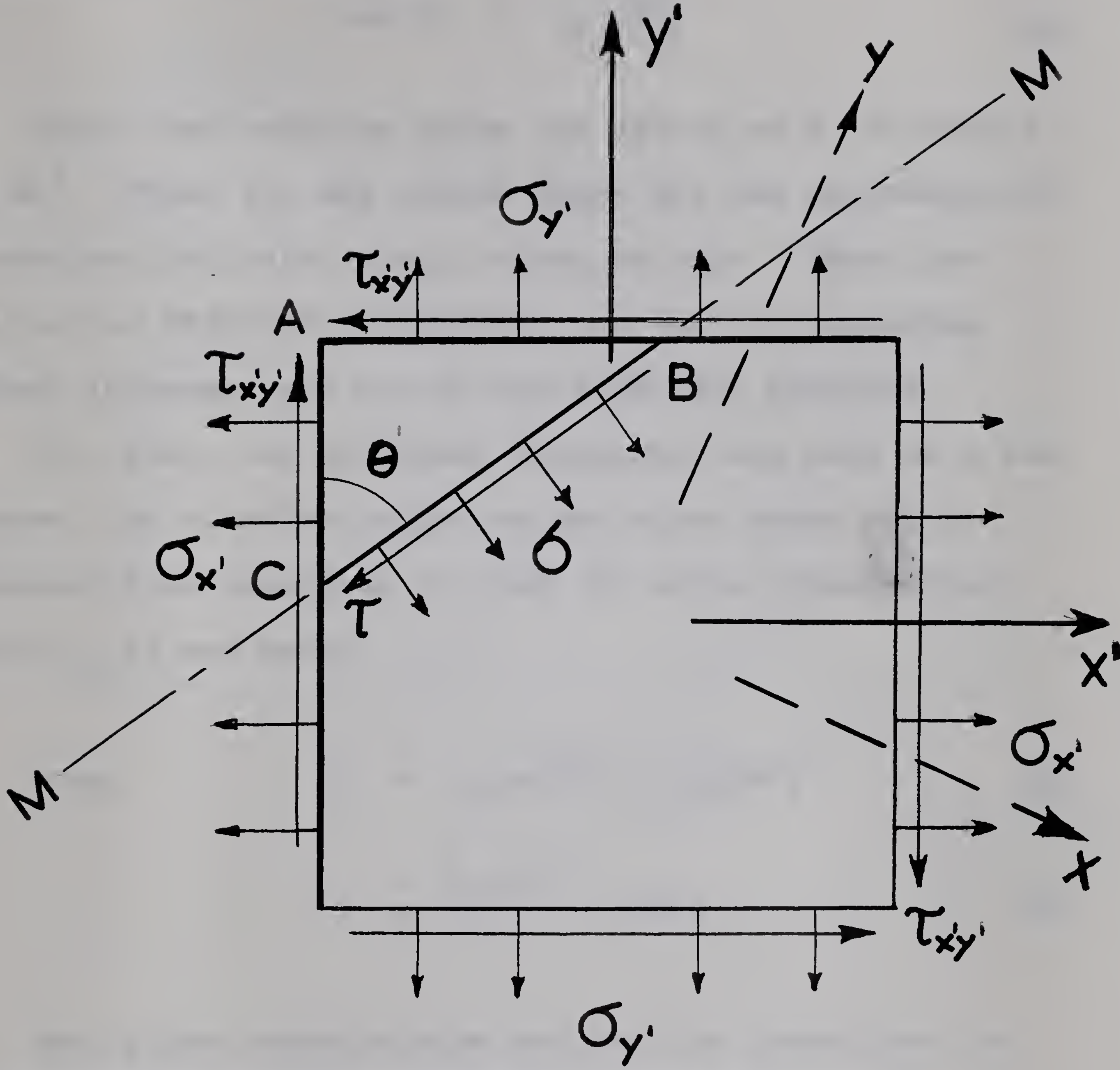
y'
y
M
$\sigma_{y'}$
$\tau_{x'y'}$
A
B
$\tau_{x'y'}$
θ
$\sigma_{x'}$
C
τ
σ
x'
$\sigma_{x'}$
M
x
$\tau_{x'y'}$
$\sigma_{y'}$

FIGURE I

For certain values of θ', τ will be zero. This gives a condition from which

$$\tan 2\theta' = \frac{2\tau_{xy}}{(\sigma_x - \sigma_y)} \qquad (5)$$

This last equation gives two values of θ', differing by 90°. Thus, for any system there are two perpendicular directions for which shear stress is zero. These are called the PRINCIPAL DIRECTIONS and the corresponding normal stresses, are called the PRINCIPAL STRESSES.

If, then, the principal directions are used as x and y axes, the stresses acting on any other plane may be obtained from equations (3) and (4) above (remembering that τ_{xy} is now zero).

Thus
$$\sigma = \sigma_x \cos^2\theta + \sigma_y \sin^2\theta \qquad (6)$$

$$\tau = \frac{(\sigma_y - \sigma_x)}{2} \sin 2\theta \qquad (7)$$

Any plane stress system may thus be identified in terms of its principal stresses, σ_x and σ_y.

These stresses may conveniently be expressed graphically by use of MOHRS CIRCLE. See Figure II.

This is a convenient means of expressing equations (6) and (7). On a plane, at an angle θ to the principal direction x, the normal and shear stresses are represented by the coordinates of point A on the diagram.

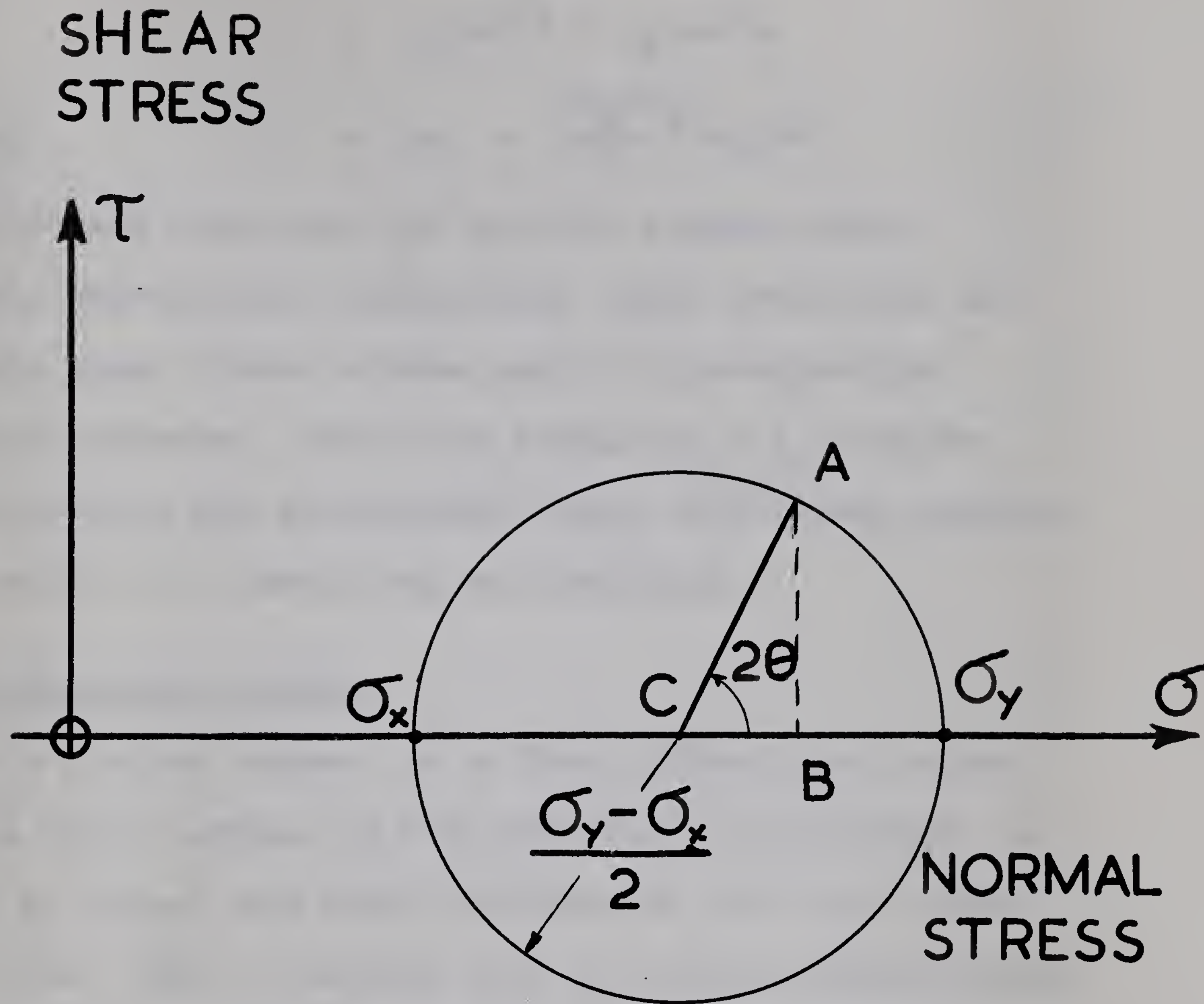

FIGURE II

Thus $\sigma = OB$

$$= OC + CB = \frac{\sigma_x+\sigma_y}{2} + \frac{\sigma_y-\sigma_x}{2}\cos 2\theta$$

$$= \sigma_x\cos^2\theta + \sigma_y\sin^2\theta$$

and $$\tau = AB = \frac{(\sigma_y-\sigma_x)}{2}\sin 2\theta$$

which are equations (6) and (7) respectively.

This construction facilitates rapid conversion between any plane stress system and its corresponding principal stresses. Since the factor $(\sigma_y - \sigma_x)$ may be determined from the photoelastic data, the stress pattern at any point in a lamina may be specified.

<u>Three Dimensional Systems</u>

In a similar manner, in a three-dimensional stress field, a cubic element of the body will be subjected, in general to normal and shear stresses on its faces. However, if the cube is located with its faces perpendicular to the three principal directions, no shear stresses will act on its sides and it is subjected only to principal stresses.

In this investigation, since the tooth is irregular and the loads are applied in several planes, the directions of the principal stresses are unknown and vary from point to point in the slice. Relative values of stress difference - as between models of various shapes - at a given point can then be found but the absolute values at a point are indeterminate.

Chapter 3

ELEMENTARY THEORY OF PHOTOELASTICITY

Detailed explanations of the optical theory explaining photoelastic phenomena may be found in Coker and Filon[14] and in Frocht.[4] A review of these follows to aid in the understanding of the present work.

Light is a periodic electromagnetic disturbance which is propogated through space, as waves on the surface of water, in the form of a transverse vibration. The vector representing the disturbance is at right angles to the axis of the ray of light. A beam of ordinary light may be considered as a composite of a large number of individual rays, each of which has its own plane of vibration. Ordinary light thus has vibrations in a random distribution in all directions.

A beam of light, in which all the vibrations lie in one plane, is said to be POLARIZED, and the plane in which the vibration occur is called the PLANE OF POLARIZATION. Such a beam may be obtained by passing ordinary light through certain crystalline materials which orient the random vibrations into one plane (or, at least, permit only certain vibrations to pass, absorbing vibrations in all other planes). This device is called a POLARIZER - in this investigation a thin sheet of POLAROID, mounted between sheets of glass for protection, was used. [POLAROID is a

suspension of needle shaped crystals of quinine idosulphate in a transparent plastic base, the crystals being oriented by stretching the sheet while cooling.]

In 1814, David Brewster(15) discovered that a brilliant color pattern could be observed in a sheet of glass under stress when viewed in polarized light. Further experiments showed that the same effect could be observed in many other transparent materials - notably certain types of plastic. The velocity of light varies with the stress in the material. This phenomenon forms the base of the science of photoelastic investigation.

Plane Polarization

The most simple type of polarization may first be considered. A ray of light is passed through a polarizer to produce a plane polarized ray. The vibration of the light ray is simple harmonic in nature and may be represented by a transverse displacement vector, S.

Now $S = a\cos\beta \cos(2\pi ft)$

where a represents the amplitude of the displacement.

f represents the frequency of vibration.

t represents the time.

β represents an arbitary angle, by which the plane of polarization may be defined. Normally β is

placed equal to zero so that
the equation reduces to

$$S = a \cos 2\pi f t.$$

Consider now this plane polarized ray as it passes through a plane sheet of photoelastic material, called the model. The plane of the model is perpendicular to the axis of the polarized ray. This shown in Figure III. The ray DO strikes a small element of the model, abcd, at O, the plane of polarization intersecting abcd along OA, at an angle α to OX. The model is subjected to principal stresses σ_x and σ_y.

If OA represents the amplitude, a, of this vibration, it may be resolved into components x and y parallel to the principal axes

$$x = a \cos\alpha \cos 2\pi f t$$
$$y = a \sin\alpha \cos 2\pi f t \qquad (1)$$

If σ_x and σ_y differ, as, in general they will, these two components will move through the model at different velocities and will thus arrive at the far face at different times. If V_x, V_y are the respective velocities and t_x, t_y the times of transit through the sheet, clearly

$$t_x = \frac{w}{V_x}, \; t_y = \frac{w}{V_y}$$

Since the two rays are transmitted without change of form, the component emerging at a given time, t, will be

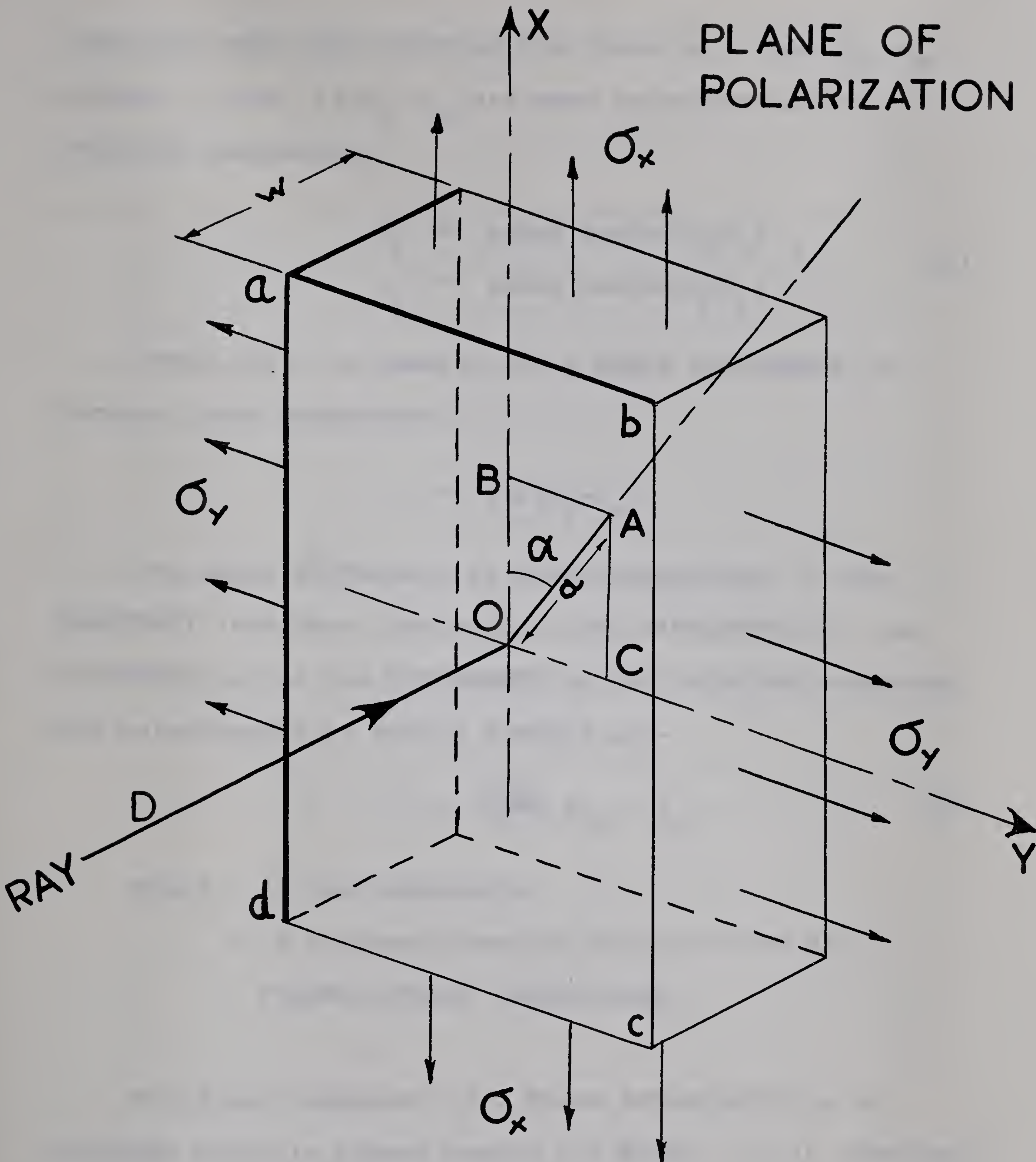
X
PLANE OF
POLARIZATION
w
σ_x
a
b
σ_y
B
A
α
a
O
C
D
RAY
d
c
σ_y
Y
σ_x

FIGURE III

identical with that entering the plate at a time t_x, t_y, earlier. Thus, if x_1, y_1 are used to represent the emerging components,

$$\left.\begin{aligned} x_1 &= a\cos\alpha \cos 2\pi f(t_2 - t_x) \\ y_1 &= a\sin\alpha \cos 2\pi f(t_2 - t_y) \end{aligned}\right] \qquad (2)$$

There will, in general, be a PHASE DIFFERENCE, Δ, between these components

$$\Delta = 2\pi f(t_y - t_x)$$

The phase difference is also proportional to the FREQUENCY (and thus inversely to the WAVELENGTH, λ), the THICKNESS and to the DIFFERENCE of the PRINCIPAL STRESSES. The relationship is easily derived as:-

$$\Delta = \frac{2\pi wC}{\lambda} (\sigma_x - \sigma_y) \qquad (3)$$

where λ is the wavelength

C is a proportionality factor called the STRESS OPTICAL COEFFICIENT.

The final component of a PLANE POLARISCOPE is an ANALYZER which is placed beyond the MODEL. It is identical with the POLARIZER and transmits only rays of light vibrating in a specified plane.

Suppose the model is removed from the Polariscope. A beam of ordinary light is polarized in the Polarizer and has a known plane of polarization. When this beam of polar-

[illegible] λ_e, λ_o [illegible]. Then, if n_e, n_o are the [illegible] the following [illegible],

(10) $$\begin{cases} \lambda_e = [illegible] \\ \lambda_o = [illegible] \end{cases}$$

[illegible] a phase difference δ between these components

$$\delta = 2\pi d(n_e - n_o)$$

The phase difference is also proportional to the frequency [illegible] the [illegible] of the [illegible]. The relationship is usually written as:

(11) $$\delta = \frac{2\pi d}{\lambda}(n_e - n_o)$$

where λ is the wavelength,

d is [illegible]

[illegible]

The [illegible] is [illegible]

[illegible]

ized light strikes the Analyzer, it will be transmitted without loss if, and only if, the ANALYZER is set with its plane parallel to that of the Polarizer. If the angle between these planes is slowly increased, the intensity of the emergent beam will steadily decrease, until, at 90° no light at all is transmitted. The Polarizer and Analyzer are now said to be CROSSED and the state is described as DARK FIELD ILLUMINATION.

Suppose the model is now replaced, with Polarizer and Analyzer CROSSED. Consider emergent components of light ray from model [x_1 and y_1 from equations 2] as they reach the Analyzer. See Figure IV.

Equations 2 may be rewritten as

$$\left.\begin{aligned} x_1 &= a\cos\alpha\cos 2\pi f(t_2 - t_x) = a\cos\alpha\cos\Psi \\ y_1 &= a\sin\alpha\cos 2\pi f(t_2 - t_y) = a\sin\alpha\cos(\Psi-\Delta) \end{aligned}\right] \qquad (4)$$

where, for compactness, $\Psi = 2\pi ft + \text{constant}$.

x_1, y_1 are represented in Figure IV by OB and OC respectively. DOE represents the plane of polarization of the analyzer (perpendicular to that of the polarizer). The ray transmitted by the analyzer is thus represented by the sum of the projections of x_1 and y_1 into DOE, i.e.

$$\begin{aligned} OD - OE &= x_1\sin\alpha - y_1\cos\alpha \\ &= a\sin\alpha\cos\alpha\cos\Psi - a\sin\alpha\cos\alpha\cos(\Psi-\Delta) \\ &= \frac{a}{2}\sin 2\alpha\left[\cos\Psi - \cos(\Psi-\Delta)\right] \\ &= -a\sin 2\alpha\sin\left(\Psi-\frac{\Delta}{2}\right)\sin\frac{\Delta}{2} \qquad (5) \end{aligned}$$

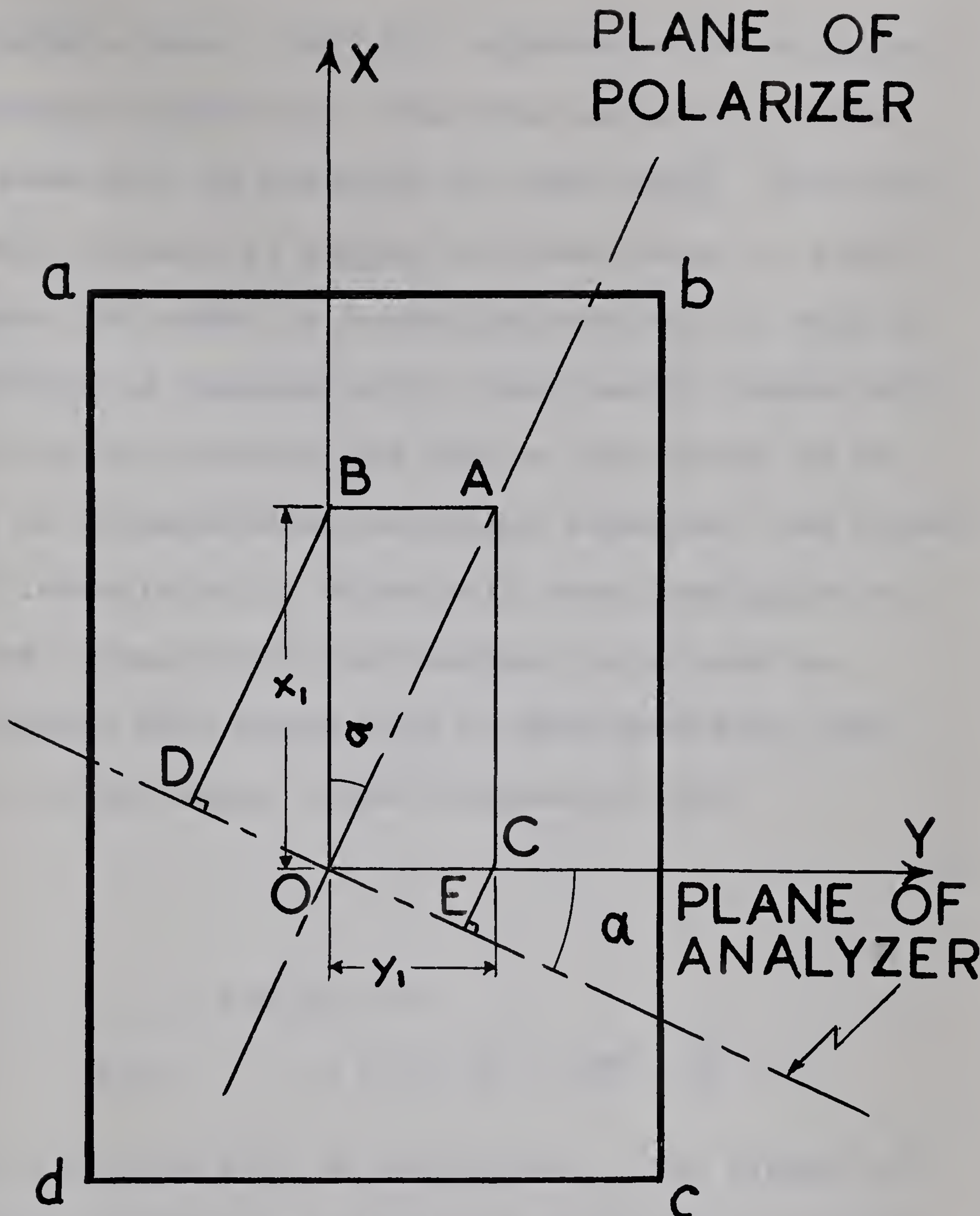
X
PLANE OF
POLARIZER
a
b
B
A
x_1
α
D
C
Y
O
E
α
PLANE OF
ANALYZER
y_1
d
c

FIGURE IV

The middle term, $\sin(\Psi-\frac{\Delta}{2})$, represents the original simple harmonic vibration. Thus the intensity of the emergent beam will be governed by $\sin 2\alpha \sin\frac{\Delta}{2}$. The intensity will be zero if <u>either</u> of these terms is zero.

Suppose the model is loaded in some way so that a stress pattern is induced in it. Any small element of the model can be isolated and can be considered to be subjected to perpendicular principal stresses, the directions and intensities of which will vary from point to point. The intensity of the emergent polarized ray passing through that point will be determined by the values of the two major terms in equation (5).

<u>Case I</u>

$$\sin 2\alpha = 0$$

$$\text{i.e.} \qquad \alpha = 0,\ 90^\circ,\ 180^\circ,\ \frac{n\pi}{2} \ldots.$$

This condition will be satisfied if the planes of polarization of both the polarizer and analyzer (which are CROSSED) parallel the planes of the principal stresses. The directions of the planes of polarization are quite arbitary and may be changed by rotating polarizer and analyzer through equal angles so that they remain crossed. There will be some points in the model at which the principal directions are parallel to the polarization planes of polarizer and analyzer. At these points α is zero, $\sin 2\alpha$ is zero and thus the intensity of the beam is zero. Thus these points will appear black and will form a pattern of lines across the field. These lines are called

the ISOCLINIC for $\beta =$ ZERO and may be plotted.

The polarizer and analyzer may then be rotated through some angle, say 10°, and a new Isoclinic plotted for $\beta = 10^\circ$. This procedure is repeated until a 90° arc has been traversed when the patterns will be found to repeat. The set of Isoclinics may then be used to derive the PRINCIPAL STRESS TRAJECTORIES.

Case II

$$\sin\frac{\Delta}{2} = 0$$

Then $\Delta = 2n\pi$, where n is any integer

But $\Delta = \frac{2\pi wc}{\lambda}(\sigma_x - \sigma_y)$ from eqn. 3

$$\text{Thus } (\sigma_x - \sigma_y) = \frac{n\lambda}{wc} \tag{6}$$

If monochromatic light is used, λ, w and c are all constants and $(\sigma_x - \sigma_y)$ is proportional to n.

Thus, at any point where $(\sigma_x - \sigma_y) =$ ZERO (principal stresses equal), n is also ZERO and thus $\sin\frac{\Delta}{2}$ is zero. These points will thus be seen as black points or lines. Similarly, another series of lines will be seen passing through all points at which $n = 1$; these are called the FRINGES OF THE FIRST ORDER.

FRINGES OF THE SECOND, THIRD, and other orders are similarly formed and form a family of lines called ISOCHROMATICS. Observation of these two families of curves, together with knowledge of the actual stresses at specific points, enables the STRESS PATTERN to be determined

throughout the model.

If white light is used to illuminate the model λ is NOT constant and the resulting patterns are more complicated. Instead of a series of black lines seen on a white background, coloured bands are seen instead. While spectacular for demonstration purposes, they are of little value for quantitative work since actual stress levels are more difficult to observe. However, white light was used to determine the zero fringe points $\left["(\sigma_x - \sigma_y)" = \text{ZERO} \right]$ on many slices. At points where the stress difference is zero a black point or line will be seen. As one moves away from the zero fringe a series of colored bands are seen, becoming more pale as the fringe order increases.

Thus, if a fairly highly stressed section is examined in polarized white light, black lines will only be seen at points where the stress difference is zero. These points can then be marked on the monochromatic pattern and identify the zero fringes positively.

Circular Polarization

As has been stated above, in monochromatic light, two sets of black bands may be observed in the field of the polariscope - the ISOCLINICS and the ISOCHROMATICS. Since these could be confused with one another, it is common practice to suppress the ISOCLINICS by modifying the apparatus. A CIRCULAR POLARISCOPE is used for this purpose; this consists of the components previously described plus two

QUARTER WAVE PLATES placed on either side of the model. These are further sheets of Polaroid, identical with the POLARIZER except that their thickness is such that the retardation through them is one quarter of a wave length (for a given wavelength of incident light).

Consider a beam of polarized light striking a quarter wave plate so placed that α is 45° [the plane of polarization of beam is at 45° to the axes of polarization of the plate]. This is shown in Figure V. Equations (4) may be used to describe the emergent beam, since this plate is equivalent to a uniformly stressed model.

Thus

$$
\begin{aligned}
x_1 &= a \cos 45^\circ \cos\Psi = \frac{a}{\sqrt{2}} \cos\Psi \\
y_1 &= a \sin 45^\circ \cos(\Psi - \frac{\pi}{2}) = \frac{a}{\sqrt{2}} \sin\Psi
\end{aligned}
\qquad (7)
$$

A vector moving with these displacement components moves in a circle and such a beam of light is described as CIRCULAR POLARIZED. (More strictly, the tip of the vector describing this beam moves in a helix about the axis of the beam).

The components (7) lie along the axes of polarization of the quarter wave plate. Figure IV must now be modified to reflect this change; see Figure VI. In Figure VI, the beam of circularly polarized light has its axis perpendicular to the plane of the drawing. It strikes the model at 0. The planes of polarization of the beam are indicated by x_1 and y_1, which are at angle α to the principal directions x and y.

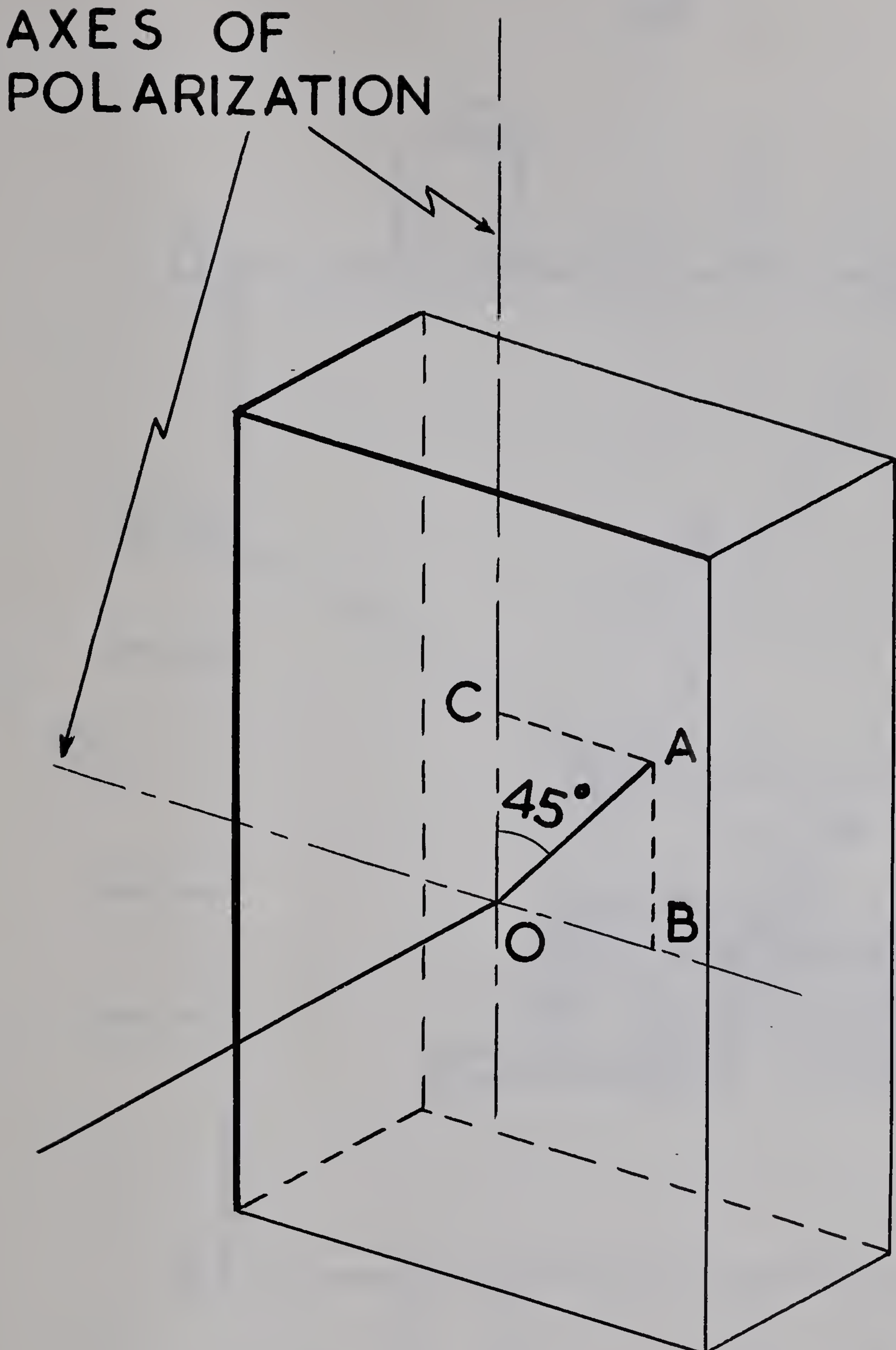

FIGURE V

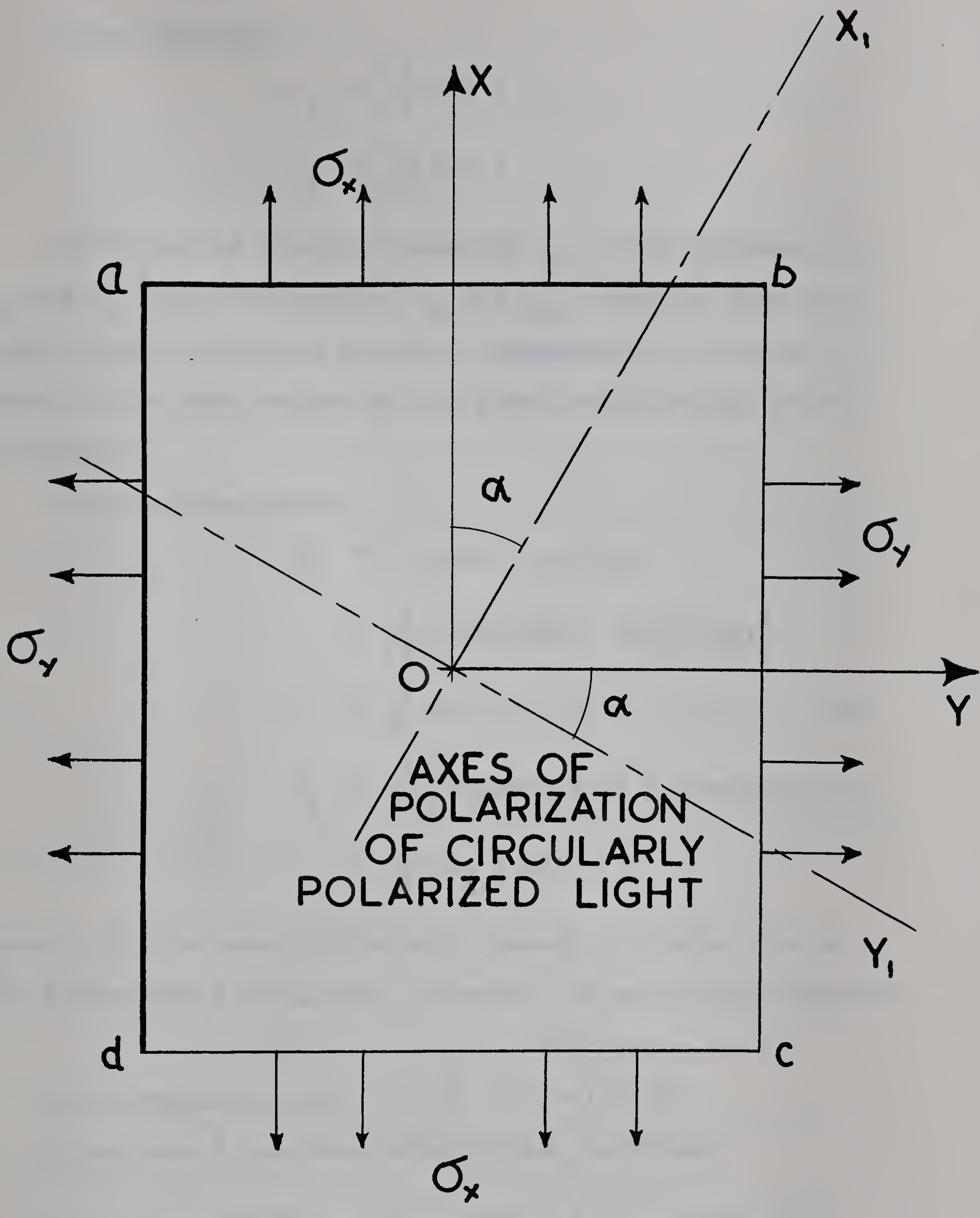

X
X1
σx
a
b
c
d
α
σy
O
Y
Y1
AXES OF POLARIZATION OF CIRCULARLY POLARIZED LIGHT

FIGURE VI

From equations 7

$$x_1 = \frac{a}{\sqrt{2}} \cos \Psi$$

$$y_1 = \frac{a}{\sqrt{2}} \sin \Psi$$

These may be resolved parallel to the directions of σ_x and σ_y. The components, x_2 and y_2, emerging from the model (after suffering relative retardation Δ) may be found by the same method as for plane polarization using equations 4.

This process yields

$$\begin{aligned} x_2 &= x_1 \cos\alpha - y_1 \sin\alpha \\ &= \frac{a}{\sqrt{2}} \left[\cos\Psi\cos\alpha - \sin\Psi \sin\alpha \right] \\ &= \frac{a}{\sqrt{2}} \cos\ (\Psi + \alpha) \qquad (8) \\ y_2 &= \frac{a}{\sqrt{2}} \left[\sin\alpha\cos(\Psi-\Delta) + \cos\alpha\sin(\Psi-\Delta) \right] \\ &= \frac{a}{\sqrt{2}} \sin\ (\alpha+\Psi-\Delta) \end{aligned}$$

where Δ is the phase difference through the model due to the difference in principal stresses, as previously defined.

For simplicity, put $b = \frac{a}{\sqrt{2}}$, $\Psi' = (\alpha+\Psi-\frac{\Delta}{2})$

Equations 8 can then be modified, to become

$$\begin{aligned} x_2 &= b\cos(\Psi'+\tfrac{\Delta}{2}) = b\left[\cos\Psi'\cos\tfrac{\Delta}{2} - \sin\Psi'\sin\tfrac{\Delta}{2}\right] \\ y_2 &= b\sin(\Psi'-\tfrac{\Delta}{2}) = b\left[\sin\Psi'\cos\tfrac{\Delta}{2} - \cos\Psi'\sin\tfrac{\Delta}{2}\right] \end{aligned} \qquad (9)$$

These two equations represent TWO superimposed circular motions, one of radius b $\cos\frac{\Delta}{2}$ clockwise and the second of radius b $\sin\frac{\Delta}{2}$ anticlockwise.

Since a change of the axes from which these circular motions are measured will merely result in a change of the phase angle Ψ' by some constant, equations 9 can be further simplified when considering the passage of these two components through the second quarter wave plate and analyser.

Taking the first the <u>clockwise</u> component, it may be written as

$$x_3 = b \cos \frac{\Delta}{2} \cos \Psi_1, \quad y_3 = b \cos \frac{\Delta}{2} \sin \Psi_1$$

where $\Psi_1 = 2\pi ft$ + CONSTANT (different from constant used on page 19)

On passing through the quarter wave plate, the emergent components may be written as

$$x_4 = b \cos \frac{\Delta}{2} \cos \Psi_2, \quad y_4 = b \cos \frac{\Delta}{2} \sin (\Psi_2 - \frac{\pi}{2})$$

$$= -b \cos \frac{\Delta}{2} \cos \Psi_2$$

the constant in the definition of Ψ having changed once again.

Finally, at the analyzer, whose axes of polarization are set at 45° to the axes of the two quarter wave plates (and at 90° to the Polarizer), the emergent ray will be of the form

$$S = b \cos\frac{\Delta}{2} \cos\Psi_2 \cos 45^\circ - b \cos\Psi_2 \cos 45^\circ \cos\frac{\Delta}{2}$$

$$= \text{ZERO for all } \Psi_2$$

Thus the clockwise circular component is extinguished.

Now, consider the anticlockwise component, which may similarly be written as

$$x_3 = -b \sin\frac{\Delta}{2} \sin\Psi_3, \quad y_3 = -b \sin\frac{\Delta}{2} \cos\Psi_3$$

These are modified on passing through the quarter wave plate and become

$$x_4 = -b \sin\frac{\Delta}{2} \sin\Psi_3, \quad y_4 = -b \sin\frac{\Delta}{2} \cos\left(\Psi_3 - \frac{\pi}{2}\right)$$

$$= -b \sin\frac{\Delta}{2} \sin\Psi_3$$

In the final transformation, the emergent beam from the analyzer is of the form

$$S = -b \sin\frac{\Delta}{2} \sin\Psi_3 \cos 45^\circ - b \sin\frac{\Delta}{2} \sin\Psi_3 \cos 45^\circ$$

$$= -\frac{2b}{\sqrt{2}} \sin\frac{\Delta}{2} \sin\Psi_3$$

$$= -a \sin\frac{\Delta}{2} \sin\Psi_3$$

As in the plane polariscope, the $\sin\Psi_3$ term represents the harmonic vibration of the beam itself. The amplitude of the emergent beam thus depends on the single term $\sin\frac{\Delta}{2}$ (see Case II, page 22 and equation 6 may be

used to evaluate the ISOCHROMATICS so formed. The sin 2α term in equation (5) is now absent and thus the Isoclinics have been suppressed.

The application of this theory may now be described. A model is made of the component to be investigated, in the form of a crossection of uniform thickness, or of the entire part if it is of uniform thickness. This model is then placed in a polariscope as shown in Figure VII.

The light source can be either white light or monochromatic. The light is passed through a diffusing screen so as to produce uniform light over a wide area, or is passed through a condenser to provide a focussed beam. In this case a lens is used beyond the analyzer to form an enlarged image on a screen, for viewing. This arrangement, which is called a Projection Polariscope, is not shown in the diagram.

The light then passes through the Polarizer and a Quarter Wave Plate, to produce circularly polarized light, after which it strikes the Model which is held in a Loading Frame. Finally, the light passes through a second Quarter Wave Plate and the Analyzer, after which it may be viewed by eye, or, allowed to enter a camera for photographic record. A typical Transmission Polariscope is shown in Figure VII.

The Polariscope is adjusted, by crossing the polarizer and analyzer and setting the quarter wave plates at 45° to them, after which the model is inserted and should appear

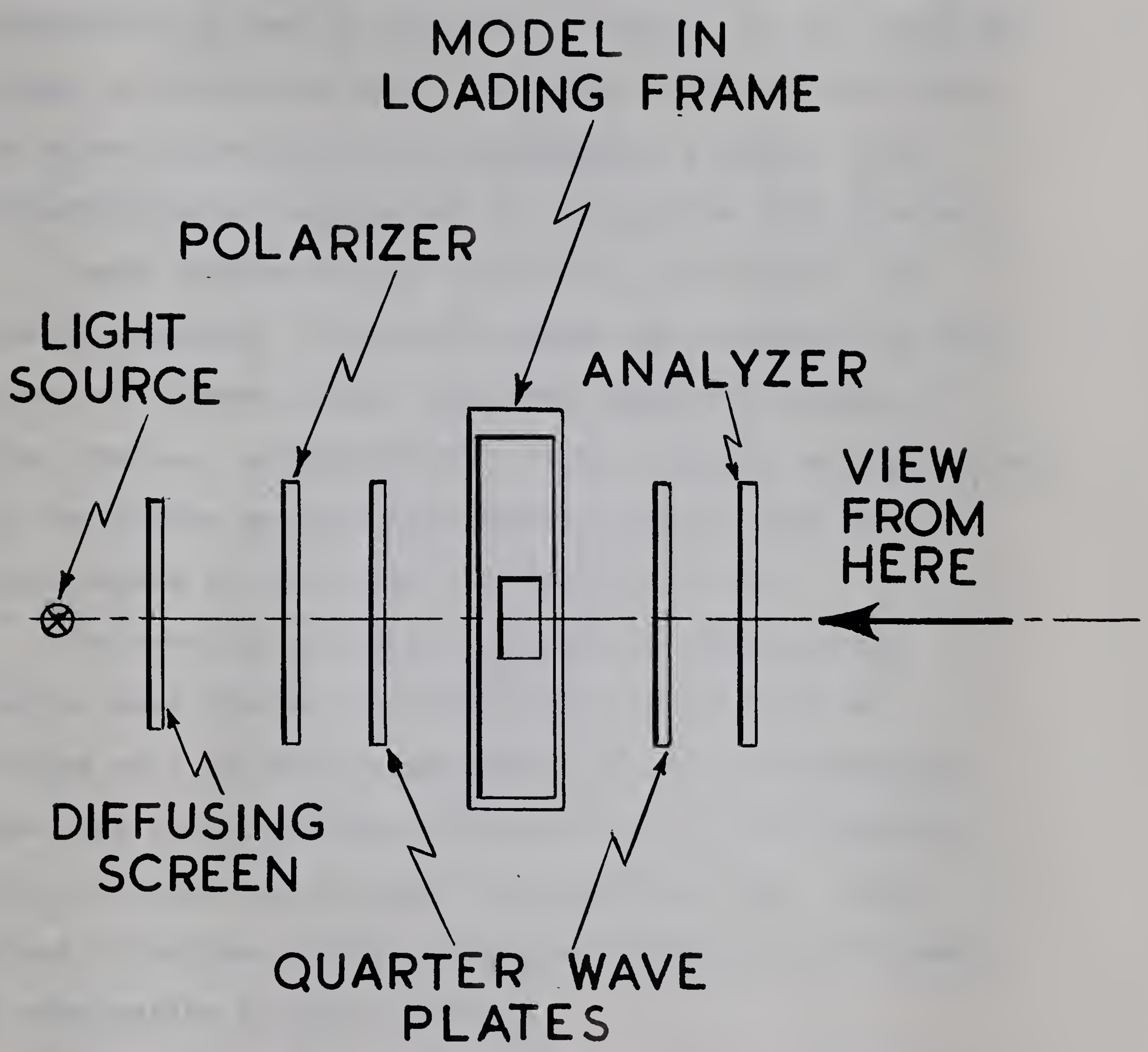
MODEL IN
LOADING FRAME
POLARIZER
LIGHT
SOURCE
ANALYZER
VIEW
FROM
HERE
DIFFUSING
SCREEN
QUARTER WAVE
PLATES

FIGURE VII

black when unloaded (since $(\sigma_x - \sigma_y)$ is zero and thus no light should pass). Loads may now be applied in two dimensions, by use of the Loading Frame. As the loads increase, a pattern of white and black areas will be seen, the black lines being the ISOCHROMATIC fringes, (the ISOCLINICS being suppressed by the quarter wave plates).

These fringes may be counted as the load is increased steadily - they will appear in succession at the points of highest stress and move toward the areas of lower stress. Alternatively, if the section is symmetrical and the stress pattern predictable, the pattern may be photographed at full load and analyzed later.

The isoclinics may be recorded by removing the quarter wave plates, in which case a second set of fringes will be seen superimposed on the isochromatics. These are the isoclinics of value $\beta = 0^\circ$ [the value is quite arbitary and is used for recording only. The actual directions of the principal stresses can be found by examination of the results.]

These fringes may be traced on a sheet of paper, photographed or otherwise recorded; the polarizer and analyzer are then rotated simultaneously through some small angle - say 15° - to change the plane of polarization and produce a new set of isoclinics for recording. This process is repeated until a total angle of 90° has been traversed, at which time the patterns will repeat. During this rotation, the isochromatics will remain

virtually unchanged and they too should be recorded.

From these fringe patterns, the principal stress values and directions - for a two-dimensional field - may be found. Methods of analysis are given in standard references.

The type of fringe pattern observed depends on the loading applied to the model. An area without fringes is subjected to uniform tensile or compressive stresses, while a series of roughly parallel fringes normally indicates an applied bending moment. At some points, many lines will come together or will form a close series of rings. These indicate points at which the stresses are high and are called stress concentrations. They are of interest to investigators since it is at these points that failures may occur.

In a specimen subjected to axial load, there will be stress concentrations at changes of section. The ratio of maximum stress at one of these points of concentration to the average stress in the minimum cross section is called the stress concentration factor.

A similar factor may be obtained by comparing the maximum stresses observed in models of differing shape when subjected to the same loading. In this investigation different shapes of filling cavity are compared in this manner.

Three dimensional stress systems may also be investigated by this same general method. The model may be placed

in the loading frame of the polariscope and the stress pattern examined under load. However, if the model be of curved shape, the resulting pattern will be distorted. In any case it will be a composite of the total photoelastic effect across the width of the model. It is for this reason that the frozen stress method has to be used to isolate the stress pattern in a particular plane of the model.

In a three dimensional system there are three principal stresses. If one of these, say σ_z, has its axis parallel to that of the polarized beam, then it will have no effect on the observed pattern. This pattern can then be treated as if it were a simple two dimensional system. In many problems the direction of σ_z is known, by symmetry or other means. The model may then be sliced perpendicular to this axis, to reduce the problem to one of two dimensions. In this investigation, the directions of the principal axes are not in general known and will certainly vary from point to point across any section.

Thus in a given section, there will be some (unknown) points at which σ_z is perpendicular to the plane of the section. At these points the stresses may be calculated. At the other points, σ_z will have some effect on the pattern of unknown amount.

Thus, in a nonsymmetrical problem such as the present one, it is impossible to arrive at an absolute value for the stresses in a section. However, relative values can be

obtained between a series of models differing only in minor dimensions. Stress concentration factors can thus be calculated, using one of the models as a standard for rating the others. This method is used to evaluate the relative merits of a variety of filling shapes in a tooth. In this case the slices contained a frozen stress pattern, so they were not loaded in the polariscope. They were merely held in a clamp which was adjustable in three planes so that the model could be placed perpendicular to the optical axis.

This arrangement is seen in Figure VIII.

FIGURE VIII

Attachment to loading frame of polariscope to hold model slice for viewing. Clamp is adjustable in three planes for alignment of slice.

Chapter 4

APPARATUS

POLARISCOPE

Several designs of polariscope were available commercially but deliveries were extended, prices were high and some were limited in capacity. Since two 13" diameter Polaroid discs, and matching quarter wave plates, were on hand, it was decided to use these and design a polariscope, having greater capacity than any available commercial machine. In particular, the large diameter of polarizer and analyzer would provide a considerable field of view and enable large models to be examined without having to move them.

The detailed drawings are attached as Appendix 'B' and the completed apparatus is shown in Figure IX. The main features are as follows:-

Chassis

This is constructed in three sections for portability. The ends are 42" high, to provide a comfortable working height, while the centre is recessed to carry the loading frame. The chassis contains shelving in cupboards for storage of weights, models, etc.

Light Source

This is mounted at the extreme left hand end of the chassis and contains white and monochromatic sources. The latter is a mercury vapour lamp (Edmunds Scientific No. 50057) and emits a mixture of wavelengths. By use of a

FIGURE IX

Transmission Polariscope,Using Circular Polarized Light. A photograph is being taken of a specimen slice.

suitable filter, a single wavelength of 5461 Angstrom units may be obtained. The bulbs are contained in a sheet metal housing to eliminate unwanted light. A diffusing screen is fitted to the front of the lamphouse to provide reasonably uniform lighting across a wide area.

Polarizer, Analyzer and Quarter Wave Plates

These are all mounted, between sheets of plate glass, in graduated rings. These rings are supported in semi-circular holders so that they may be turned to any desired angle. The holders can be mounted at varying distances along the chassis to accommodate unusual models.

Loading Frame

This frame is built as a unit so that it may be removed if necessary. It is of the guillotine type - the model being mounted inside a rectangular steel frame by suitable hangers. Load is applied by weights acting through a lever system. Several loads may be applied simultaneously and in two dimensions if required. It provides a working area over 15" square.

The frame containing the model and loading system slides in vertical guides on a base which can be moved from side to side so that any portion of the working area may be placed on the optical axis of the polariscope. Controls for these movements are provided at the viewing end of the chassis, so that adjustments may be made while watching the patterns.

The stress patterns were previously 'frozen' into the three dimensional models, and the loading frame served only to hold the slices for examination.

THREE DIMENSIONAL LOADING FRAME

Detailed drawings are attached as Appendix 'C' and the completed apparatus is seen in Figure X, with a closeup of a loaded tooth in Figure XI. As may be seen, it consists of a simple rectangular framework to carry a deadweight lever system. The tooth is loaded through an articulated plunger which carries a pressure foot, seen in detail in Figure XI. This consists of a casting of parts of the two teeth in the upper jaw opposing the one being tested. Joints at both ends of the plunger enable the teeth to be aligned correctly to give a good simulation of normal biting action.

OVENS AND TEMPERATURE CONTROL

Two Fisher "ISOTEMP Ovens" were used for casting, curing and annealing. Each had a capacity of approximately 1 cubic foot and were capable of holding a set temperature within 1 °C.

Since the annealing process required slow temperature changes, a gear box was constructed, as shown in Figure XII to drive one of the oven thermostats. The final drive sprockets could be changed to vary the heating/cooling rates, normally about 2 °F (1.1 °C) per hour was used.

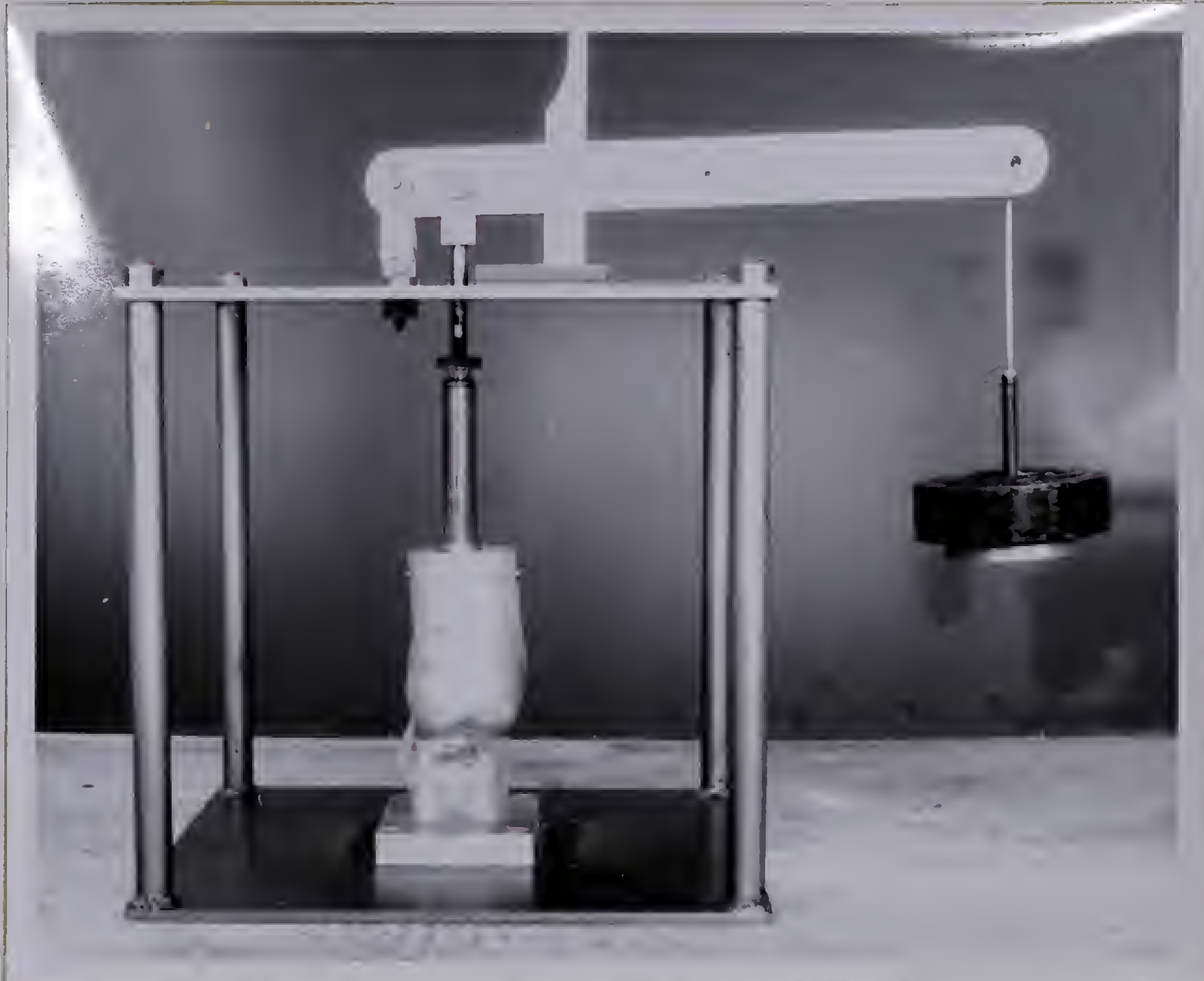

FIGURE X FIGURE XI

Loading Frame, complete with tooth, ready for stress freezing. A scale can be seen by loading arm, by which deflections are gauged. A close up of the model and the loading shoe is seen below.

FIGURE XII

Slow speed drive for oven thermostat. The motor in the foreground drives the thermostat through a Meccano gear box immersed in oil. The final drive is by chain to the sprocket wheel at the top of the picture. This is mounted on the thermostat spindle.The total gear ratio is approximately two million to one and the temperature changes at about 3 °F (1.7 °C) per hour.

MATERIALS

The major materials used in this investigation, and their suppliers, were:-

Epoxy Resin No. 2053
Hardener No. 3401
(used to make models)

Hysol (Canada) Ltd., P.O. Box 53,
Station R., Toronto, Ontario.

'Silicone Release Agent' Compound 20,
(to coat mould surfaces to prevent sticking)

Don Corning Corporation,
Midland, Michigan.

Permlastic H.B. Base and Catalyst,
(to seal mould against leaks)

Kerr Manufacturing Company,
Detroit 8, Michigan.

Silicone Oil L45
(for oil bath for stress freezing)

Union Carbide Corporation,
270 Park Avenue, New York.

Chapter 5

EXPERIMENTAL PROCEDURE

The 'standard' textbooks of photo-elasticity such as Frocht, or Coker and Filon, contain little information on three dimensional work, particularly as regards experimental technique. A major part of this work was thus devoted to the establishment of standard procedures so that duplicate models could be made of reasonably constant shape and optical quality. The methods so established are described in detail in Appendix 'A' - the following being a summary of the main steps.

It was decided to concentrate on one tooth, and one particular type of cavity, in this preliminary investigation to minimize the parameters. The tooth selected was the first mandibular molar - the sixth tooth on the right hand side of the lower jaw - and this was modified with a Class I preparation, that is, a cavity of roughly rectangular shape on the occlusal or biting surface of the tooth. Figure XIII shows a scale drawing of this tooth and cavity.

The shape and size of teeth vary considerably from person to person[16] so a model of a "typical" example was prepared six times full size in wax. From this a two part aluminum mould was prepared. The models were cast inverted, crown down. This position had two advantages - bubbles, dirt, etc. tended to rise in the mould as the plastic cured and distortion and shrinkage occurred at the tooth root.

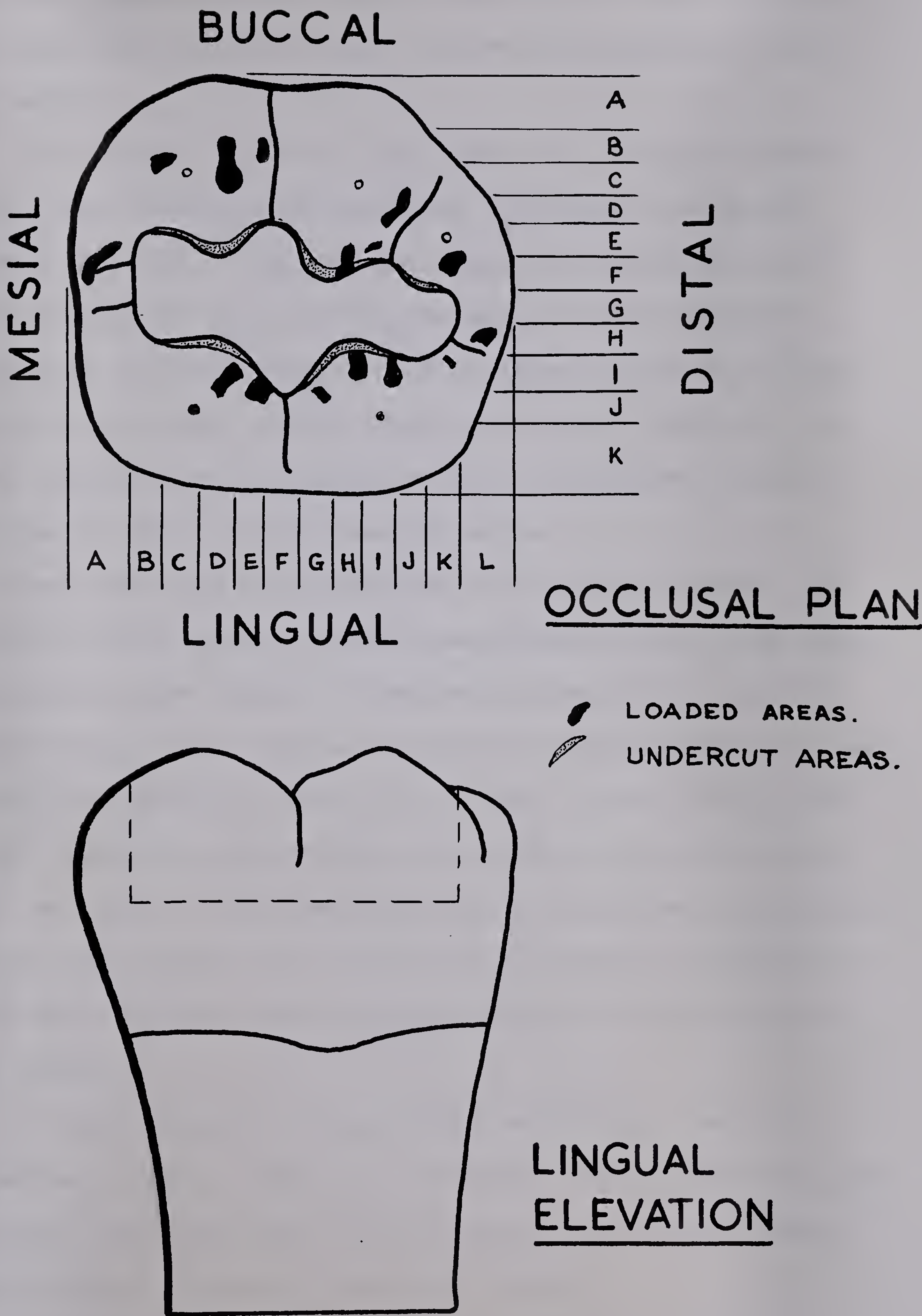
BUCCAL
MESIAL
DISTAL
LINGUAL
A B C D E F G H I J K
A B C D E F G H I J K L
OCCLUSAL PLAN
LOADED AREAS.
UNDERCUT AREAS.
LINGUAL ELEVATION

FIGURE XIII

Since the investigation concentrated on the upper half of the tooth, this gave the best chance of obtaining a fault free model.

The material used for the models was an epoxy-based HYSOL resin, supplied as resin No. 2053 and a separate hardener No. 3401. These were mixed in specified proportions and poured into the heated mould, which was then maintained at 230°F (110°C) for at least 36 hours to allow the plastic to set. After slow cooling the model was removed, polished and examined in the polariscope to check that the residual stress level was low.

The model was next machined to its final shape. The cavity in the occlusal surface was milled, using high speed cutters and slow feeds. A template maintained a uniform cavity shape. The centre of the real tooth,called the pulp, is soft and carries little or no load. Since its outline is very irregular it proved impossible to cast its shape into the model. For repeatability, an idealised rectangular section pulp chamber was used on most models, although one model was prepared with material removed to approximate a pulp cavity.

It was essential, during this machining, that the temperature rise be kept to a minimum. To achieve this end, the model was hand held and the cutter air cooled. This method proved successful and quite rapid.

Curing was the next step in the process. A batch of models was placed in an oven and their temperature slowly

raised at not more than 2°C per hour to 302°F (150°C) at which level it was held for at least three days, five or more being more usual, followed by cooling at the same slow rate.

This curing helped to relieve internal stresses generated during casting and machining and also modified the structure of the plastic, rendering it considerably harder and somewhat more brittle. A model in this state is seen in the Frontispiece.

The model was now ready for loading and "stress-freezing". The model was heated in a silicone oil bath while under load to about 270°F (130°C), the critical temperature of the plastic. At this point the plastic deformed appreciably, which was marked by a movement of the loading lever. A complex rearrangement of the molecular structure occurs and, on cooling, a stress pattern was 'frozen' into the model, when the load was removed.

The stress distribution in the model was three dimentional and could not be examined directly, even if the tooth had been of uniform section, since the fringe pattern observed was a composite of the total effect across the full depth. The final step in preparation was then to slice the model into a series of parallel plates about 3 mm. thick. The slices were cut and polished by hand and this proved to be the most tedious of all the work. It was essential not to heat the plastic, which would distort the frozen-in patterns. The slices were then ready for examination in the polariscope.

Chapter 6

RESULTS

The first part of this investigation was concerned with the techniques necessary to produce uniform models with little or no residual stress. At each stage, different methods were tried and those which gave the most satisfactory results are incorporated in the detailed procedure (Appendix 'A'). Several 'dead-ends' were investigated in this work and these may now briefly be discussed.

MIXTURE RATIO-HARDENER TO RESIN

This did not appear to be critical with up to about 60% hardener (as against the 40% recommended). Satisfactory models were obtained and there was some decrease in curing time, although it became more difficult to dissolve the hardener completely, giving a cloudy plastic which was of little use. Reducing the amount of hardener was more serious since the curing time increased - below about 20%, the models were soft and rubberlike.

CASTING ROUTINE

The temperatures seemed to be quite critical. The first few teeth were cast into a mould which had been heated for 30 minutes or less. Although the oven had regained its nominal temperature, the inside of the mould was still well below 110°C. Hence when being filled, the plastic striking

this cold surface 'froze' and turned opaque, rendering the model useless. Care should thus be taken always to pre-heat the mould adequately.

Similarly the removal of the model from the mould should not be hurried. After setting for 24 hours, the exposed surface was quite hard but the interior remained soft, so that the model collapsed when the mould was opened. Hence the casting time should never be less than 36 hours and should be increased for larger models.

PREPARATION OF MODELS

Standard workshop techniques were found to be quite satisfactory for shaping the plastic models, except that slow cutting rates are essential to prevent heating of the model. The methods used were probably too cautious, since several other investigators have used diamond tipped saw blades for cutting.[17]

However, the slow working methods used had one advantage in that they introduced no new residual stresses into the model, which would then have to be removed by annealing.

ANNEALING

The temperature of all models was raised and lowered at the same speed, about 2°F per hour. The duration of the annealing period was varied from three to ten days. The models annealed all had small residual stress fields and three days seemed to be adequate to eliminate these - no

advantage was seen in the longer periods.

LOADING AND STRESS FREEZING

It is most important that the whole tooth should reach the critical temperature in order that the loading should be correct. The plastic changes state at this temperature and becomes softer. If the core remains below the critical temperature, then the load distribution changes and an incorrect stress pattern is frozen into the model.

The model was heated in an oil bath to try to obtain even and uniform heating - the oil being stirred mechanically. Two models were fitted with thermocouples placed deep in the plastic. Thermometers were also placed around the model and observed frequently during the heating cycle.

It was found that the oil temperature varied by not more than 2°F, showing that the stirring was adequate. At the beginning of the cycle, the temperature of the plastic lagged that of the oil by about 17°F. Near the critical temperature, the maximum temperature difference was 4°F. It was for this reason that the oil temperature was raised 5°F above the critical (that temperature at which a marked deformation in the model occurs) and held there for at least one hour. This ensured that all the plastic reached the critical state.

The rate of cooling appeared to have no effect on the frozen pattern, so natural cooling was normally used. The heating tank was lagged and took 8 - 10 hours to return to room temperature.

The models were identified by a number engraved on their base. The code '6L' was used to identify the tooth - the sixth in the lower jaw (on the right side) - and each model was then numbered in sequence. Two types of pulp chamber were cut, referred to as Types I or II. Type I was rectangular with sharp corners on the floor of the chamber, which was 6 mm. thick. This was used at first, but eventually discarded in favor of Type II, which was also rectangular but had rounder corners on the floor, 10 mm. thick. These bore little resemblance to the prototype but were used since it was possible to repeat these shapes to produce a series of similar models.

The numbered models, and their history, were as follows:-

6L1. First model to complete all stages successfully. It was lightly loaded - about 150 lb. - and then sectioned. Some fringes were observed and the method proved, but it was decided to increase the load on other models.

6L2. Two models were given this number, both having a type I pulp chamber. After cutting these two had no residual stress patterns so they were loaded

and heated to critical temperature <u>without</u> being annealed. This proved disastrous as both collapsed-the first after half an hour with 1022 lb. load, and the second after 45 minutes with 522 lb. This showed the necessity of annealing the models. Large temperature differences were found in the oil tank while loading these models and the stirrer was then added.

6L3. Pulp Chamber Type I. This model was used to check for temperature gradients in the model. A small hole was drilled through the buccal surface to lead wires to a thermocouple glued to the floor of the pulp chamber. Ceramic glue was used which involved heating the model to 250°F for two hours. For this reason and because of the hole drilled in it, 6L3 was not used to determine stress patterns. As previously stated, the temperature differences involved were quite small. Since this model was spoilt, it was used as a testpiece and was subjected to several loading cycles at different loads, times and temperatures.

The next four models were loaded with a variety of weights and specimen slices were cut for examination. Model 6L4 was loaded with 622 lb. while 6L6 carried 822 lb., both having Type I pulp chambers. 6L5 (522 lb.) and 6L8 (322 lb.) had Type II pulp chambers. After examination of these models,

it was decided to standardize on Type II pulp chambers and a constant load of 422 lb. Each model was carved with a modified Class I cavity as described below. The only exception was 6L111, in which a natural pulp chamber was carved.

The remaining models were as follows:-

6L7. Slightly enlarged cavity. Buccolingual section.

6L9. Cavity had parallel sides and rounded corners. Mesiodistal section.

6L10. Cavity had undercut walls and rounded corners. Buccolingual section.

6L11. A natural pulp chamber was carved into this model, but became oversize during shaping. It was thus rejected, drilled to take a thermocouple and used with 6L3 to check critical temperatures.

6L111. Natural pulp chamber. Standard cavity with parallel walls and square corners. Buccolingual section. Replaced 6L11 in sequence.

6L12. Cavity with parallel walls and continuously curved floor with no corners. Buccolingual section.

6L13. Cavity with parallel walls and sharp corners. Buccolingual section.

6L14. No cavity cut in this model which thus represented the natural, undecayed state. Buccolingual section.

6L15. Cavity with parallel walls and sharp corners. Mesiodistal section. Forms a pair with 6L13.

6L16. Cavity with parallel sides and rounded corners. Buccolingual section. Forms a pair with 6L9.

6L17. Cavity with parallel sides and sharp corners, but deeper than standard cavity (as in 6L13). Buccolingual section.

To summarise the above, otherwise identical models were cut having cavities with:-

(a) parallel walls, sharp corners-6L13, 6L15.
(b) parallel walls, rounded corners-6L16, 6L9.
(c) parallel walls, continuously curved floor-6L12.
(d) undercut walls, sharp corners-6L18.
(e) undercut walls, rounded corners-6L10.
(f) no cavity at all-6L14.

plus three other models, all with a type Class I cavity (parallel walls, sharp corners):-

(g) wider cavity than standard-6L7.
(h) deeper cavity than standard-6L17.
(i) natural pulp chamber-6L111.

These final eleven models (7,9,10,111,12 to 18) were then sliced as indicated above. Figure XIII shows an occlusal plan of the tooth and indicates the approximate planes of sectioning. It must be emphasized that it was extremely difficult to cut identical sections from the various teeth, since the saw tended to wander.

Table 1 shows the correspondence of the sections in the various models. The sectioning planes shown in Figure XIII refer to models 6L15, 6L13 and 6L16 - this table identifies similar sections in the other teeth.

Table 1

MESIODISTAL SECTIONS

MODEL											
6L15	A	B	C	D	E	F	G	H	I	J	K
6L9	A	B	C	D	E	F		G	H	I	J

BUCCOLINGUAL SECTIONS

6L13	A	B	C	D	E	F	G	H	I	J	K
6L16	A	B	C	D	E	F	G	H	I	J	K
6L18	A			C		E			G		
6L17	A		B	C	D	E		F	G		
6L111	A			C	D	E			G		
6L12	A			C		E			G		
6L14	A			C	D	E			G		
6L17	A			C		E			G		
6L10	A			C		E			G		

Models 6L13, 6L15 and 6L16 conform to the standards shown in Figure XIII. For other models, the sections shown above were cut and conform, in vertical columns, to the sections cut in models 6L13, 6L15 and 6L16.

On some teeth, only a few sections were cut to economise on time and effort - the uncut blocks were saved for further examination if necessary. Figures XIV and XV show some of the sections laid out in rows. Model 6L16, for example, was completely sliced and the sequence of slices clearly shows how the tooth, and cavities, change section along its length.

The stress pattern in each slice was photographed for ease of examination. Some of these patterns are examined below while the remainder are collected in Appendix 'D' and are available for further study.

The following sets of photos may be examined in sequences for comparison:

SET ONE - Figure XVI

EFFECT OF ARTIFICIAL PULP CHAMBER

The upper photograph shows 6L13E with an artificial pulp chamber and the lower 6L111D with a 'natural' chamber. It will be noticed that the stress patterns, in the contact areas of the two teeth, are very similar, showing that the two models and slices are comparable. In the central area, of course, there are considerable differences although even here there are similarities, the patterns at the right side being quite alike. The material in the 'bulge' between the pulp horns does little to strengthen the model and stress concentrations are evident at the cavity corners in both models and at the tips of the horns in 6L111D.

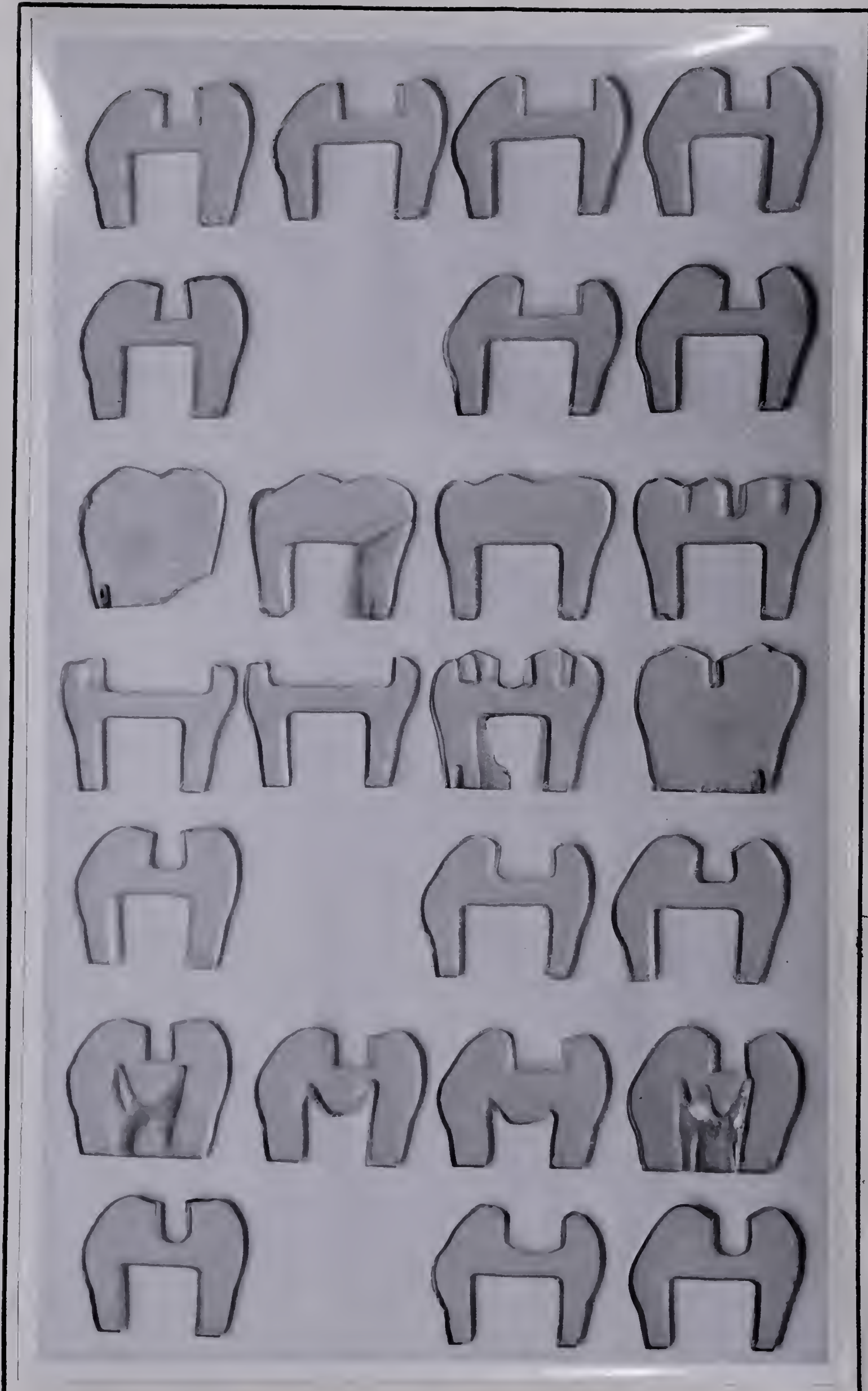

FIGURE XIV

Slices of tooth

Models Set 1.

FIGURE XV

Slices of tooth

Models Set 2.

FIGURE XVI

SET ONE

Comparison of stress patterns in models with artificial and natural pulp chambers.

It would appear that the use of an artificial pulp chamber has not affected the load distribution greatly but has naturally modified the stress distribution at the base of the cavity. However, even here the pattern of distribution is similar and changes in stress concentration due to changes in the cavity shape should be capable of comparison.

SET TWO - Figure XVII

A CENTRAL SECTION

This set of nine pictures shows similar sections through an untouched tooth and eight cavities of various types. Perhaps the most remarkable feature is the similarity of pattern, in the areas remote from the cavity, in seven of these nine sections. Only 6L12E and 6L17E show a major difference on the left hand side and these two form a pair in themselves. Their difference is perhaps due to a slight change in plane of sectioning or loading. When the possible variations in shaping, curing, stress-freezing and sectioning are considered, such reproducibility indicates that the recommended method is quite satisfactory.

The zero points $\left["(\sigma_x - \sigma_y)" = \text{zero} \right]$ are marked on these photos - these were obtained as described on page 23 above. Some of these are rather surprising - particularly those adjacent to the left hand corner of the cavity in 6L13F, 6L16F, 6L18E and 6L111E. However, looking at the right hand corner of the cavity and counting fringes from the upper right face, where there is a zero fringe, 6L13F

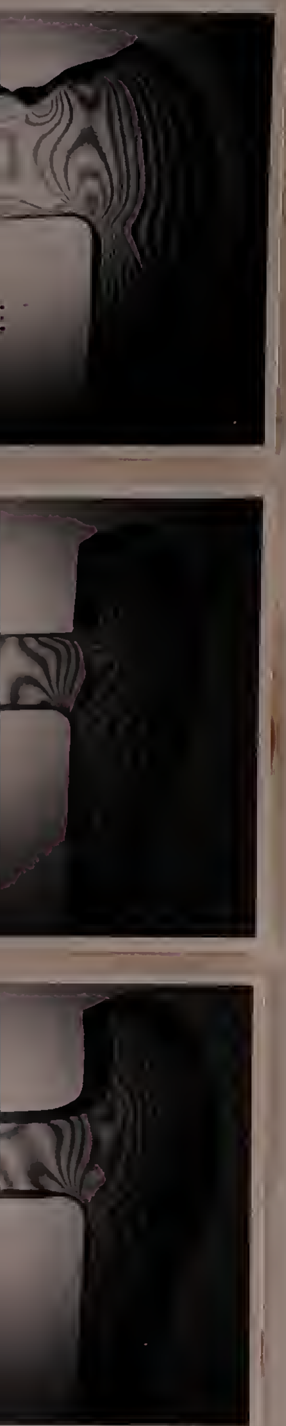

FIGURE XVII

SET TWO

Comparison of stress patterns in central sections of models having a variety of cavities.

(sharp corner) reaches 11 fringes, whereas 6L16F (round corners) reaches only 8 fringes, a clear reduction of stress concentration. However, 6L12E (round floor) should score even lower if judging by the normal principles governing stress concentrations at sharp corners. In fact, 11 fringes can be counted. On the other hand the two models with undercut walls - 6L18E, sharp corners, 10 fringes; and 6L10E, rounded corners, 8 fringes - are in agreement. Similarly, 6L7E, 10 fringes, and 6L17E, 11 fringes, tend to corroborate these figures and render it likely that 6L12E suffered local damage during shaping or perhaps was 'burnt' during the polishing. The slice from the normal pulp chamber, 6L111E records 7 fringes at this point - the lowest of all values - but its section is much thicker than any other.

SET THREE - Figure XVIII

A MESIAL SECTION

This set of nine slices are taken from the same teeth as the previous set. Eight of these sections exhibit very similar patterns away from the cavity - the pulp horn in 6L111C modifying the last pattern. The effect of increasing the radius of the base of the cavity, with parallel sides, is again confused. 6L13D, square cornered, reaches 11 fringes on the right and 9 on the left; while the rounded corner model 6L16D, drops to 8 on the right but remains at 9 on the left. The round based cavity, 6L12C, remains at 8 on the right but

FIGURE XVIII

SET THREE

Comparison of stress patterns in mesial sections of models having a variety of cavities.

increases slightly at the left to 10. However, the undercut models do show a clear improvement. The square cornered 6L18C with maxima of 14 and 11 considerably exceeds the values of 6L10C which reaches 8 in each of its rounded corners.

The two nonstandard rectangular cavities also agree, within limits, with the above values. 6L111C is quite interesting in that it shows fairly high concentrations - about 9 - not only in the corners of the cavity, but at the head of each pulp horn.

SET FOUR - Figure XIX

A DISTAL SECTION

This series of eight slices again shows reasonable correspondence between the various stress patterns away from the cavity.

Taking first the parallel sided cavities, once again the left corner does not correspond to expectations while the right hand corner does exhibit a reduction in stress concentration with increase in radius [6L13I, sharp, 13: 6L161, round fillet, 11, and 6L12G, curved base, 10]. The left hand corner, by comparison seems hardly to be stressed at all. The undercut cavity exhibits the same effect with a sharp corner value of 15 (6L18G) reducing to 11 when rounded (6L10G).

Once again 6L7 and 6L17 corroborate these findings.

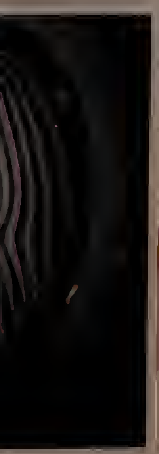
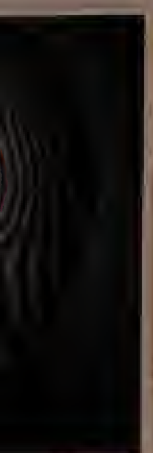

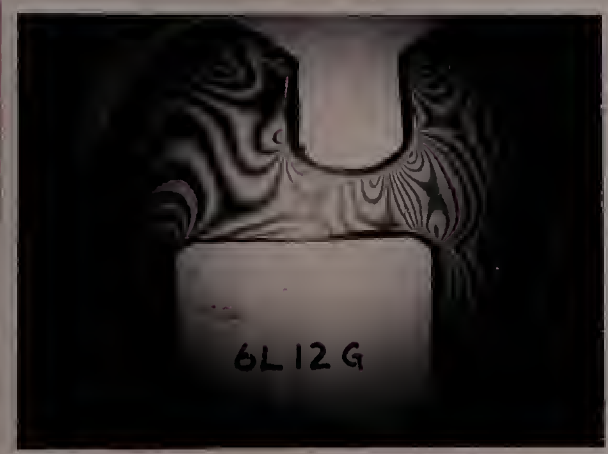

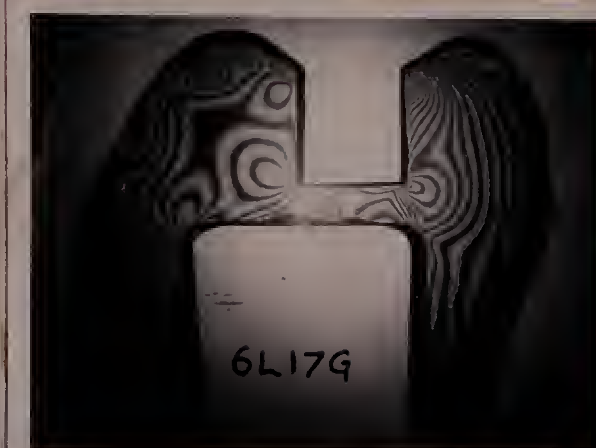

FIGURE XIX

SET FOUR

Comparison of stress patterns in distal sections of models having a variety of cavities.

These results are summarised in Table II. At each section the maximum number of fringes observed at the right hand corner of the standard cavity - model 6L13 - is taken as the average value. The stress concentration factors for the other models are then expressed as a percentage of this chosen standard.

Table II

MODEL		MESIAL SECTION	CENTER SECTION	DISTAL SECTION
6L13	Sharp Corner	100	100	100
6L16	Round Corner	73	73	92
6L12	Curved Floor	73	100	83
6L18	Undercut, Sharp Corner	127	91	125
6L10	Undercut, Round Corner	73	73	92
6L7	Wide Cavity	100	91	117
6L17	Deep Cavity	82	100	83
6L111	Natural Pulp Chamber	82	64	-

STRESS CONCENTRATION FACTORS FOR SELECTED SLICES
AS PERCENTAGES - STANDARD CAVITY = 100%

Numerically, these results are not conclusive but they do exhibit a trend, which agrees with that to be expected from normal engineering practice. Stress concentrations will always be found at sudden changes of section. These can be reduced by modifying the design to include a rounded

fillet. As the radius of the fillet increases the stress concentration decreases. At the right corner of the cavity this principle is fairly well illustrated, the factor reducing successively as the radius increases. The only exception is 6L12F and the discrepancy here may be due to inaccurate cutting or loading, or to 'burning' during slicing operations.

Also, when this corner was undercut, the factor increased in two of the three sections, as was expected. Rounding this undercut corner decreased the stress concentration factor appreciably in all cases.

Previous Work in this Field.

The first record discovered of the use of photoelasticity in dental research describes work carried out by Noonan in 1949.[5] He used sheets of 1/4" Bakelite shaped to represent an idealised buccolingual section. Three types of cavities were tested - parallel sides and rounded corners, parallel sides with a semicircular base and undercut with rounded corners. The cavities were filled with standard dental amalgam and then loaded centrally. The results obtained are listed below in Table II.

TABLE II

RESULTS FROM NOONAN[5]

Parallel sides, rounded corners	3 2/3 fringes
Parallel sides, rounded base	4 2/3 fringes
Undercut sides, rounded corners	4 fringes

These are maximum fringe values observed in floor of cavity.

These results are not directly comparable with those from this investigation, as the sections are idealised and symmetrical. The rounded base cavity had the highest fringe order which does not conform with the present results. This may be due to the method of loading which was symmetrical and differed radically from that used in this investigation. It is more realistic to include a filling material, which must play some part in carrying the load. However, it would have been better to have applied the biting forces to the tooth as well as to the filling.

The papers by Granath[2] and Castaldi[3] discuss the types of failure found after modifying teeth with a Class II preparation. Generally, this is larger than the Class I type discussed in this work and extends to the mesial or distal surfaces of the tooth. No photoelastic techniques are discussed and the approach is qualitative.

The papers by Haskins,[6] Guard,[7] and Mahler[8] all use photoelastic techniques in two dimensions. Slices of plastic were shaped to represent sections of the FILLING in a Class II preparation and these were supported on soft metal blocks which represented the remainder of the tooth. These were then loaded and the stress patterns in the filling compared for various shapes. Mahler measured the actual deformations of the slice at various points. From these readings $(\sigma_x + \sigma_y)$ could be obtained. Since $(\sigma_x - \sigma_y)$ can be obtained from the isochromatics, both principal stresses could be calculated. While interesting applications of

photoelastic techniques, these investigations pursue a different approach from that followed in the present work, and the results are thus not comparable.

Finally, two papers by Granath[(9), (18)] provide some results of interest. Once again, Class II preparations were discussed, and a two dimensional technique was used. Slices of epoxy resin were prepared to represent a somewhat idealised buccolingual section with four shapes of cavity, - parallel sides, round corners; parallel sides, rounded base; undercut with rounded corners and short undercut walls with a continuously curved base forming the greater part of the section.

In addition, some of the cavities were filled with a modified epoxy resin. The ratio of the moduli of elasticity of the model tooth and filling corresponded to the ratio of the moduli of dental amalgam and dentine, the major constitutent of the human tooth. In these models the pulp chamber was idealised in a similar way to that used in the present investigation, except that the walls were not parallel but tapered inwards.

As in Noonan's paper, the loads were applied symmetrically and results for the four sections are recorded below in Table III.

TABLE III

RESULTS FROM GRANATH[18]

Parallel sides, rounded corners	5 fringes
Parallel sides, rounded base	12
Undercut, rounded corners	6
Semicircular section	9

(These fringe values are counted from the fringe patterns printed in the paper, and may be in error due to losses in reproduction.)

These results contradict those found in the present investigation. The difference in this case is clearly due to the method of loading, which was applied through a cylindrical pressure foot bearing on the sloping faces of the tooth on either side of the cavity. These forces acting outward at about 45° from vertical, impose a bending moment on the floor of the cavity. Since the rounded base section has a floor only 2 cm. thick while the others are 4 cm. (the semicircular section is 3.5 mm. thick), this explains the variations in fringe orders. Since the loadings are so dissimilar, little comparison can be made between these results, and those of the present investigation.

These previous investigations have all chosen to make a two dimensional investigation by modelling a slice of the tooth. They have also all used an idealised section and a method of loading which has enabled complete solutions of the stress pattern to be obtained. The present investigation has used a more realistic shape (except for the pulp chamber)

and method of loading. The stress patterns so obtained probably more closely represent the actual situation than those reviewed. However, because of their unsymmetrical nature, they are very difficult to analyse to determine specific stress levels.

A small element within the tooth will have three principal directions and be subjected to three principal stresses. Only rarely will one of these principal directions be perpendicular to the plane of slicing. At most points, the principal directions will <u>not</u> lie in the plane of the section.

At these points equation 3, (page 18)

$$n = \frac{2\pi wC}{\lambda} (\sigma_x - \sigma_y)$$

no longer applies. Instead, some more complicated equation, of the form

$$n = \frac{2\pi wC}{\lambda} \Big(f_1(\sigma_x) + f_2(\sigma_y) + f_3(\sigma_z) \Big)$$

must be used. The three functions of the principal stresses vary from point to point, according to the orientation of the principal directions relative to the slice. It is for this reason that, in this investigation, no absolute values have been calculated. Relative values between similar models are quoted since it is felt that geometric similarity will cause the stress patterns to be of similar shape, point for point.

The whole process of slice production is complicated, and contains many steps at each of which an individual model could deviate from standard. A difference of one fringe order between any two models is thus probably not significant. This may explain some of the inconsistent results in the present investigation.

Perhaps a model tooth could be made with a slice of birefringent plastic embedded in a non-birefringent plastic, such as perspex. When loaded, the stress pattern in the slice could then be observed directly and compared with those obtained in this investigation.

In view of all these uncertainties, all that may be said is that the present investigation indicates that the shape of the cavity is significant. Care should be taken to round the corners of the base of the cavity, and to finish it smoothly so as to reduce the maximum stress level as far as possible.

Chapter 7

CONCLUSIONS

(1) The method of manufacture described in this investigation has produced satisfactory plastic models free of residual stress.

(2) The techniques established during this investigation for modifying the castings and producing finished models with low residual stress have proved reliable and repeatable.

(3) Minor modifications to the shape of the cavity can make considerable reduction in the stress level in critical areas of the tooth. If the stress concentration factor of a standard sharp corner cavity be taken as 100%, then the use of rounded corners can reduce the stress factor by up to 25%. On the other hand an undercut cavity with sharp corners, often advocated to retain the filling more solidly, increases the factor by about 25%. The use of cavities with rounded corners thus reduces maximum stress level and would probably increase the filling life.

Chapter 8

RECOMMENDATIONS

If further work is done in this field the following points should be considered for investigation:-

1. Natural Pulp Chamber. An artificial shape of chamber was deliberately chosen for this work for ease of manufacture. It is felt that this choice has not vitiated the results but that the use of a more realistic shape would be even more satisfactory. Thought should be given to casting the chamber into the model although this will raise considerable technical problems, because of its tapered shape.

2. Presence of Filling Material. The models used in this investigation all were loaded with empty cavities, although in practice the filling material would provide some assistance in supporting the load. Consideration should be given to filling this cavity with some material to simulate actual conditions more closely. If the filling were represented by a birefringent plastic, some interesting results regarding the stress concentrations in the filling might become available.

3. Theoretical Solution. The results are almost entirely qualitative due to the complex three dimensional stress

system set up in the model. It would be most useful if a three dimensional relaxation method could be established to evaluate the principal stresses at a network of points through the model working from values obtained from sets of mutually perpendicular sections. This would probably require the use of a computer.

REFERENCES

(1) BLACK, G.V., Operative Dentistry, 1908 Medico Dental Publishing Co.

(2) GRANATH, L.E. Preparation Av. Klass II, Kaviteter, Mjolktandbettet, Odontologisk, Revy, 10: 257, No. 3, 1959.

(3) MacRAE, P.D., ZACHERL, W., and CASTALDI, C.R., A Study of Defects in Class II Dental Amalgam Restorations in Deciduous Molars, J.C.D.A. 28: 491, August 1962.

(4) FROCHT, M.M. Photoelasticity, 2 vols. 1941 and 1948.

(5) NOONAN, M.E. The Use of Photoelasticity in a Study of Cavity Preparation, J.Dent. Child 16:28, 4th Quarter 1949.

(6) HASKINS, R.C., HAACK, M.S., and IRELAND, R.L., A Study of Stress Pattern Variations in Class II Cavity Restorations as a Result of Different Cavity Designs. J. Dent. Res. 33: 757, December 1954.

(7) GUARD, W.F., HAACK, D.C. and IRELAND, R.L., Photoelastic Stress Analysis of Buccolingual Sections of Class II Cavity Restorations, J.A.D.A. 57:631, November 1958.

(8) MAHLER, D.B. Analysis of Stresses in a Dental Amalgam Restoration. J. Dent. Res., 37: 516, June 1958.

(9) GRANATH, L.E. Further Photoelastic Studies on the Relations Between the Cavity and the Occlusal Portion of Class II Restorations. Odontologisk Revy 15: 290, No. 3, 1964.

(10) WHEELER, R.C., A Textbook of Dental Anatomy and Physiology, 3rd Edition 1962, W.B. Saunders, Philadelphia, p. 388 et. seq.

(11) IBID, p. 396.

(12) BULLETIN E-106, Photoelastic Casting Resin for Three Dimensional Studies, Hysol (Canada) Ltd. Toronto.

(13) MANTLE, J.B., Recent Advances in Experimental Stress Analysis, The Engineering Journal 44: 3, January 1961.

(14) COKER, E.G., and FILON, L.N.G., Photo-elasticity, Cambridge University Press, 1957.

(15) TIMOSHENKO, S.P., History of Strength of Materials, McGraw-Hill 1953, p. 249.

(16) WHEELER, R.C., A Textbook of Dental Anatomy and Physiology 3rd Edition, 1962., p. 240.

(17) MANTLE, J.B., United Kingdom Photoelastic Stress Analysis Laboratories, 1961, University of Sask. pages 5, 6, 7 and 8.

(18) GRANATH, L.E., Photoelastic Model Experiments on Class II Cavity Restorations of Dental Amalgam, Odontologisk, Revy, 16:7, Supplement 9, 1965.

Appendix 'A'

DETAILED PROCEDURE FOR PRODUCTION OF MODELS

1. CASTING

(a) MOULD PREPARATION

The interior surface of the mould was first cleaned and polished to remove any debris left from previous work. Since most deposits were inflammable, they were usually burnt off with an oxy-acetylene flame, leaving a soft carbon deposit which could then easily be removed with a wire brush and cloth, leaving a well polished surface. This was found to be quite important if good models were to be obtained.

The surface of the entire mould was then brushed with DOW CORNING "Silicone Release Agent" and placed upside down in a FISHER ISOTEMP oven set at 150°C (302°F), where it was left for about 3 hours. Surplus release agent was drained from the tooth during this baking process - if left in the mould, this discoloured the vital crown area of the model.

The mould was in two parts, clamped together with long bolts. It was found that the joint needed careful sealing as the resin when poured, was very fluid and leaked readily, spoiling the cast and fouling the inside of the oven, where it set to a hard glass-like skin which defied all attempts at removal. KERR PERMLASTIC was found satisfactory for sealing. This rubber-based sealing compound, supplied as a separate BASE and CATALYST, which have to be mixed just

before use, was applied liberally on the outside of the mould and worked into the groove around the joint surface. The mould was then replaced in the oven and preheated for about an hour to 110°C (230°F) to equalise its temperature for casting.

(b) PLASTIC PREPARATION

While the mould was preheating, the plastic could be prepared. As mentioned earlier a HYSOL epoxy-based resin was used, supplied in two parts. The resin (plastic) - HYSOL 2053 - is a clear, honey-coloured, viscous syrup, while the hardener - HYSOL 3401 - is a white granular substance.

HYSOL recommended that 40 parts, by weight, of hardener be added to 100 parts of resin and this proportion was used for all models. The accuracy of proportioning did not seem critical as some preliminary trials were made with hardener proportion varying from about 30% to 100%. Above about 60%, the resulting plastic lost its transparency and became opaque - at the lower end of the scale curing times increased considerably and the models were soft and rubbery.

A suitable amount of resin and hardener were weighed out in beakers. The models used in this work required about 200 grams of resin - and 80 gms. of hardener - but a little extra was used to ensure a full mould. Any surplus was poured into a simple rectangular mould to provide a test specimen if required.

The hardener was then placed in the oven with the mould to preheat, while the beaker containing the resin was placed in an oil bath and heated to between 150° and 160°C [302 - 32°F].

(c) CASTING

This step was complicated by the need to hold the temperature of the mould to quite fine limits. If the mould was below about 100°C (212°F) the plastic "froze" and crystallised on its surface during pouring and produced a useless model. The solubility of the hardener in the resin also decreased rapidly as the temperature fell; on the other hand HYSOL specified that the temperature of the mix should not exceed 115°C (239°F).[11]

The mixing and casting thus had to be done rapidly. As soon as the resin reached 150°C (302°F), and assuming that the mould was stabilised at 110°C (230°F), the hardener was removed from the oven and poured into the resin, mixing being aided by rapid stirring with a thermometer. The temperature of the resin fell rapidly, as the hardener was added, to the 110-115°C range (230° - 239°F). Some fumes were evolved at this time and care had to be taken to avoid breathing them. The hardener dissolved rapidly to produce a clear liquid. If necessary any small specks of dirt were removed and the plastic poured steadily into the mould, which was <u>not</u> removed from the oven for this purpose. The mould was filled almost to its brim, after which the beaker and

any surplus was placed in the oven and left for about ten minutes. The mould was then checked for leakage, topped up if necessary and any remaining plastic poured into an auxiliary mould. The beakers, thermometers, etc. were then cleaned at once to remove the plastic while it was hot and soft. Hot, soapy water proved adequate for this purpose.

The mould was left in the oven at 110°C (230°F) for at least 36 hours. After 24 hours, the surface of the plastic was hard and had usually shrunk a little - the centre of the model was still liquid and it could not safely be removed from the mould. After 36 - 48 hours, the oven was turned off and left to cool naturally. When removed from the mould, the model was rough and often had flash at the joint. These were soon removed by gentle polishing and revealed a clear, transparent model. Occasionally a small air bubble or piece of dirt was observed and in one case, internal cracks developed, presumably due to internal stresses. See Figure XX.

II. SHAPING PROCESSES

These may all be considered together, although carried out at different stages of production, since they have much in common. Since the ultimate use of the model was to observe stress patterns due to external loading, it was obviously essential to reduce all other stress effects as much as possible. Unfortunately, the plastic was extremely

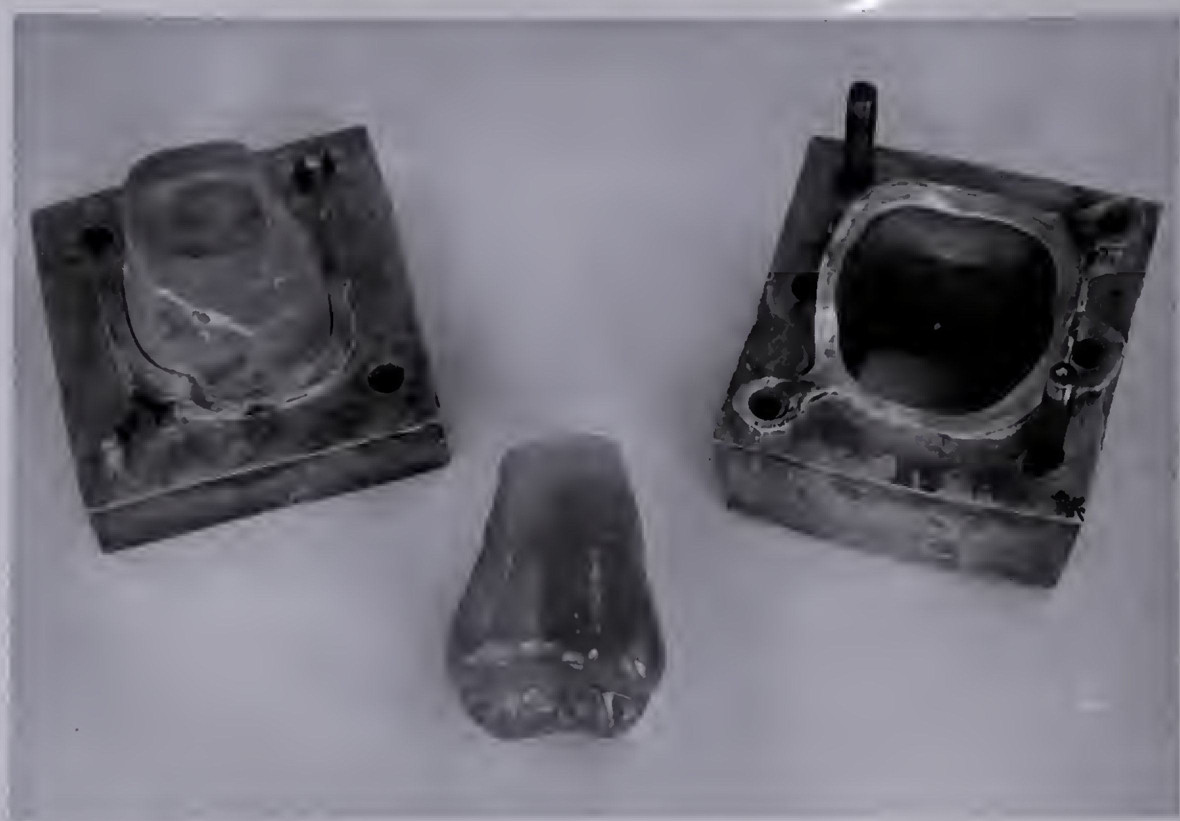

FIGURE XX

On the left side, the lower section of the mould is shown, with a new casting still in place. On the right the upper section of the mould, with its securing bolts, is shown. At the center a polished casting is seen.

sensitive to local heating. Because of its low thermal conductivity, heating induced local internal stresses which would modify the imposed patterns under investigation. Thus, all machining processes had to be done very slowly since they involve friction while cutting, and thus local heating.

The pulp cavities and preparations were largely made by milling. Tungsten carbide end mills were used in a small Unimat lathe, set up as a vertical milling machine. See Figure XXI. A plaster cast of the crown of the tooth was used to provide a firm base support for the model. This was moved by hand on a face plate to press against the milling cutter which was driven at the highest speed available on the machine - nominally 10,000 R.P.M. See Figure XXII.

The base of the tooth was first cut square by hacksaw and four holes drilled and tapped in its extreme corners. These were used to mount a sheet metal template with a cut-out to guide the shank of the milling cutter to profile the pulp cavity. Some plastic was first removed by drilling - the remainder being milled. Air was directed at the cutter to help keep the plastic cool and remove the waste plastic.

The tooth was then mounted on a steel base, which was used for locating the model in all subsequent operations. The preparation was then cut in the crown of the tooth - the template in this case being a plaster cast with a suitable hole cut into it. Use of templates ensured reason-

FIGURE XXI

Milling cavities on Unimat lathe. The model rests on a wooden base plate. The drill is fed downward by the lever seen near the top of the machine.

FIGURE XXII

Closeup of machining operation. The model tooth is hand held and slides on the wooden base. The sides of the cavity are cut by sideways pressure.

able repeatability of form - however all models required final handfinishing with knife and, or, fine files, to reproduce the finer details of shape.

After curing and "stress-freezing", the model was sliced so that the stress patterns at various sections through the model could be examined. This was done by handsawing, using an ordinary hacksaw with a fine blade. The tooth was bolted to a base block for rigidity. Vertical slotted posts mounted on this block guided the hacksaw blade to keep the cut fact reasonably plane. The assembly was then placed in a sink and the cutting done under water to ensure minimum temperature rise and distortion of the stress pattern. Although tedious this procedure was found most satisfactory as it virtually eliminated all heating of the model.

Finally, the slices were polished so that the surfaces were reasonably smooth. The sawing marks were removed on a TRIMMER, a machine used for shaping plaster models. The slice was pressed against a motor driven steel wheel with an abrasive surface similar to that on a file. The slice was supported by a recessed steel block - this helped provide uniform pressure and made it more easy to hold the slice steady. A copius supply of water kept the slice cool. See Figure XXIII. This again was a tedious operation as only light pressures could be used to minimise heating and to maintain reasonably constant thickness across the slice. The trimmer produced a matt, translucent surface

FIGURE XXIII

Polishing slices on trimmer.
The slice is supported by a recessed block so that pressure may be applied evenly.

which was then polished with a soft cloth buff. Patience was again necessary at this stage since high pressures produced considerable heat in the specimen. In Figure XXIV note how the buff was loaded with pumice powder for rough polishing.

III. CURING

HYSOL recommended that cast models be cured to reduce residual internal stresses.[11] Their bulletin implied that this should be done immediately after casting. In this investigation, however, the rough castings were considerably modified by machining which, even if carefully done, would introduce more residual stresses. Normally, therefore, the machining was done before curing although a few models were cured first, in an attempt to determine which procedure was better. It was found that there was no significant difference in residual stress level between models machined before or after curing. This was because great care was taken not to introduce residual stress during machining. However, since the plastic was appreciably harder after curing, it was found to be much more convenient to machine first and then cure, than to reverse the order.

It was felt to be more logical to eliminate residual stress as far as possible rather than to allow it to accumulate in the hope that curing would remove it eventually. It was for this reason that the machining was done slowly and that the casting techniques described above were employed.

FIGURE XXIV

Final polishing of slice.
The slice is pressed against a soft buff which is loaded with pumice powder for the rough work. Final polishing is done with a clean buff.

This caution proved most successful as most models exhibited only small amounts of residual stress.

The models to be cured were placed in a cold Fisher ISOTEMP oven and raised slowly to a temperature of 150°C (302°F) at which level they were held constant for a minimum of three full days - usually five or more - before being cooled slowly to ambient temperature. The rate of change of temperature rise or fall was held to 2°C (3.6°F) per hour. The temperature control of the oven was normally by hand operation of a thermostat, which maintained a given setting whithin 0.5°C (0.9°F). During the heating and cooling cycles, the thermostat knob was replaced by a sprocket wheel, chain driven from a compact 'MECCANO' gear box and powered by a small electric motor. Preliminary tests, using thermocouples, showed that this gave a good uniform rate of change - an essential part of the curing process.

While curing, the plastic became appreciably darker in colour, although still transparent; as previously mentioned it also became appreciably harder to machine.

IV. STRESS FREEZING

This plastic has a critical temperature at about 130°C (270°F), at which an internal molecular rearrangement occurs; it is on this phenomenon that the whole process of 'stress freezing' depends.

As the temperature of a loaded model is slowly raised to about 270°F a sudden increase of deformation and change of state is observed. The plastic becomes relatively soft and breaks easily. If the model is then cooled below the critical temperature the plastic again becomes hard and brittle but the deformation is "locked" into the model and the resulting stress pattern is 'frozen', and can be examined at leisure either by direct viewing of the whole model, or by slicing in cases where the stress is nonuniform across the thickness.

In this investigation, the loading of the model was particularly complex as there were many points of contact between mating teeth and the forces at these points acted in different directions. The first trials were done, for simplicity, with a cylindrical pressure foot, but this was soon changed to an aluminum casting of portions of the maxillary second bicuspid and first molar, the teeth normally opposing the first mandibular molar. This gave a reasonable representation of the real distribution of biting load.

The prepared model tooth was bolted firmly to the base plate of a loading frame with solid top and bottom and open sides - see Figure X. The load was applied to the model through a lever system with loose pin or ball joints which provided sufficient adjustment for alignment of the mating teeth. After the model and pressure foot were correctly aligned the whole frame was placed in a tank of

silicone oil covering the tooth to a depth of about one inch. See Figure XXV.

The oil was heated fairly slowly by an electric immersion heater to the critical temperature, a stirrer being used to equalise temperature throughout the model. Once the characteristic increase in deformation at the critical temperature was observed, the temperature was allowed to rise about 5°C (9°F) and then held constant for at least an hour. This ensured that the entire model had reached the critical temperature. The heater was then switched off and the oil allowed to cool naturally; this took several hours as the tank was insulated. The model could then be removed, cleaned of oil and prepared for examination in the polariscope.

FIGURE XXV

Stress freezing in progress. The tooth, in loading frame, is submerged in a bath of silicone oil. The stirrer is placed close to the model, the heater being across the far end of the tank. The thermostat control can be seen on side of the insulated box. The deflection of the model may be estimated by movement of the loading arm against the scale seen on top of the frame.

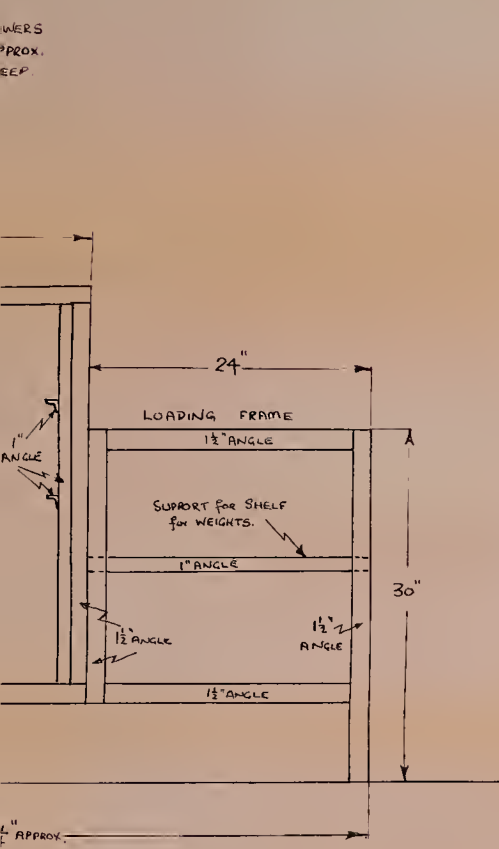

N FRAME.

ALL JOINTS TO BE WELDED

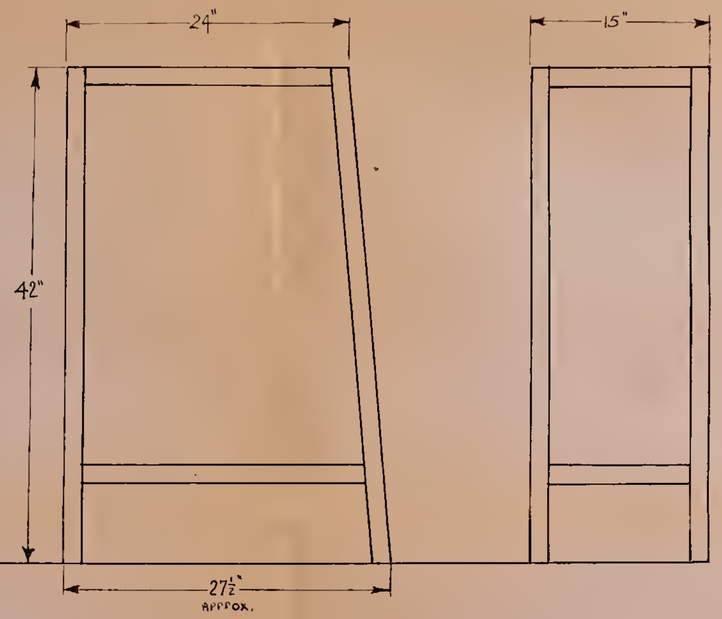

END VIEW and FRONT ELEVATION of VIEWING SUB-FRAME.

TWO FRAMES TO BE CONNECTED BY FOUR ¼" BOLTS.
IF 16 SWG SHEATHING IS PREPARED FOR THIS FRAME,
BOLT IT ON TEMPORARILY AS MOUNTING DETAILS HAVE
YET TO BE DESIGNED.

LEVELLING SCREWS ARE TO BE FITTED TO ALL LEGS
OF BOTH FRAMES.

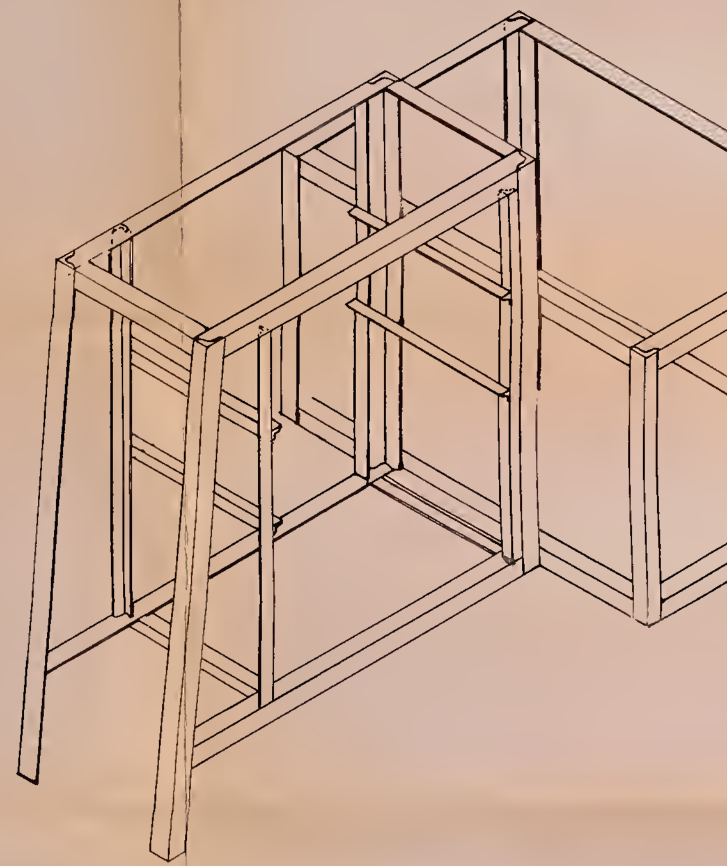

ISOMETRIC VIEW OF MAIN FRAME

POLARISCOPE FR

MECHANICAL ENGINEERING - UNIVERSITY of AL

MEJ 1001 EWJ. 8 JULY

. ARRANGEMENT
DING FRAME

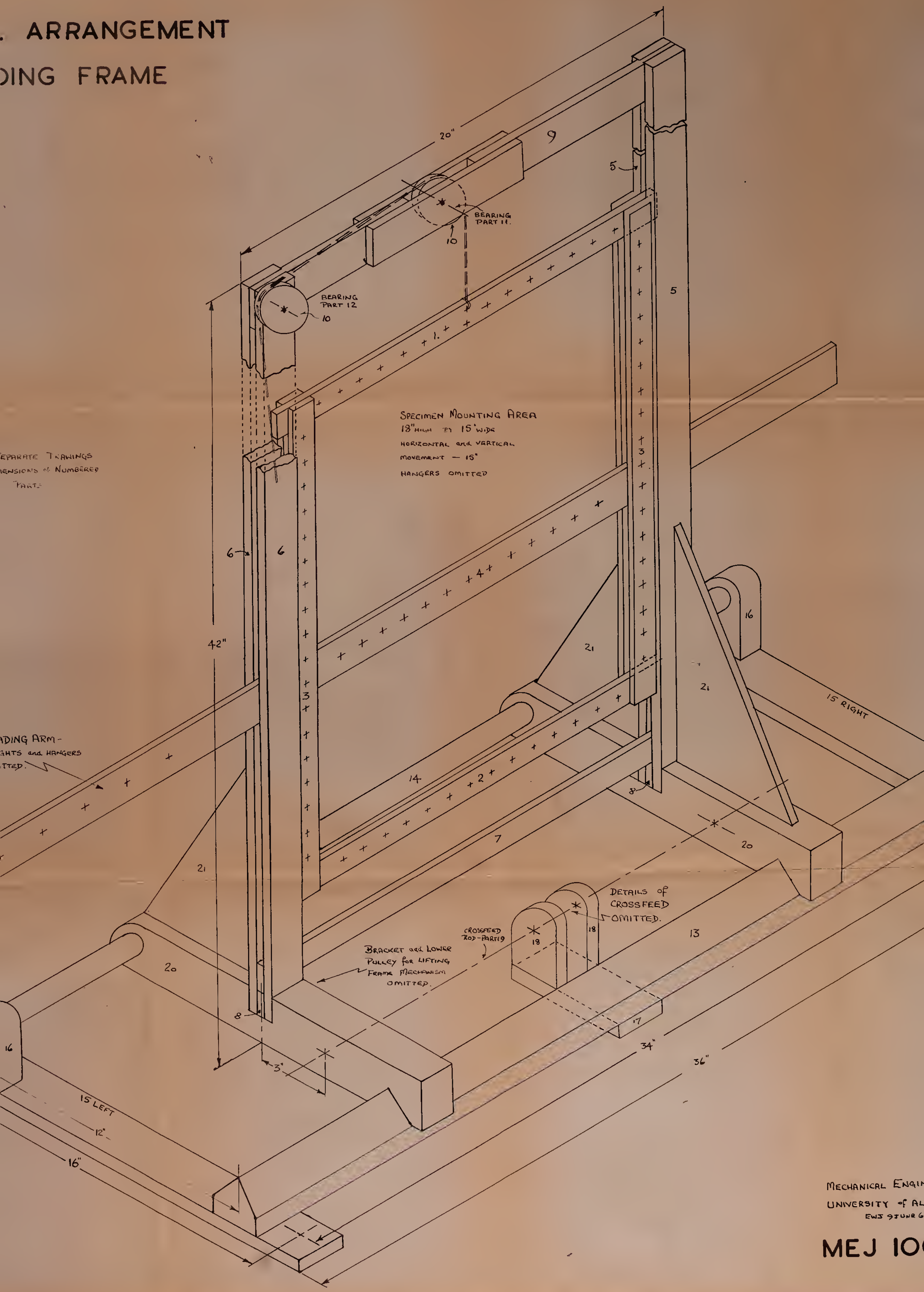

MECHANICAL ENGIN
UNIVERSITY of AL
EWS 9 JUNE 6

MEJ 10

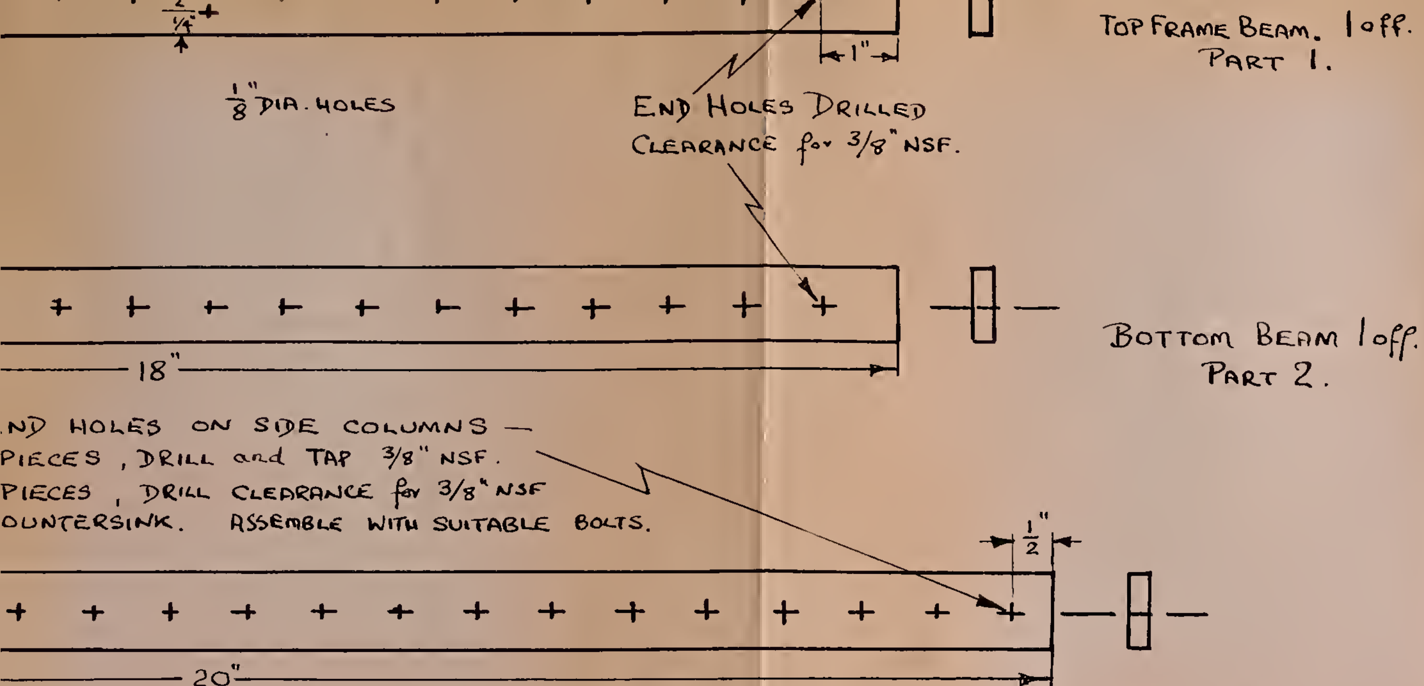

...ND HOLES ON SIDE COLUMNS —
...PIECES, DRILL and TAP 3/8" NSF.
...PIECES, DRILL CLEARANCE for 3/8" NSF
...OUNTERSINK. ASSEMBLE WITH SUITABLE BOLTS.

...S TO BE MADE from 1" x 1/4" MILD STEEL STRIP
...OLES NOT OTHERWISE DIMENSIONED 1/8" DIA ON 1" CENTRES

MECHANICAL ENGINEERING.
UNIVERSITY of ALBERTA.
EWJ 10 JUNE 63.

...ME DETAIL. **MEJ 1003**

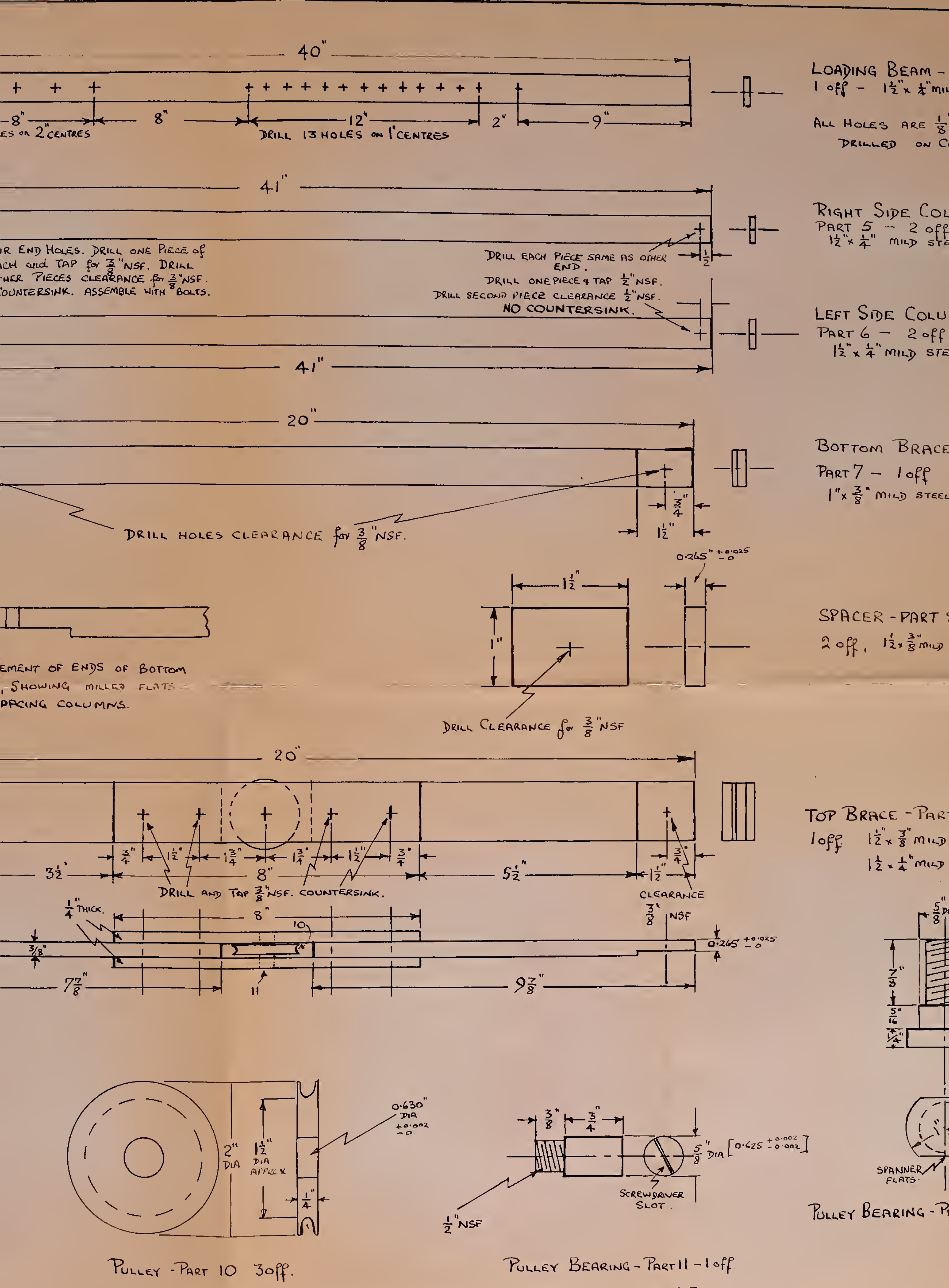

MECHANICAL ENGINEERING - UNIVERSITY of ALBERTA. EWJ 10 JUNE 63.

UPPORT COLUMN DETAILS. MEJ1004

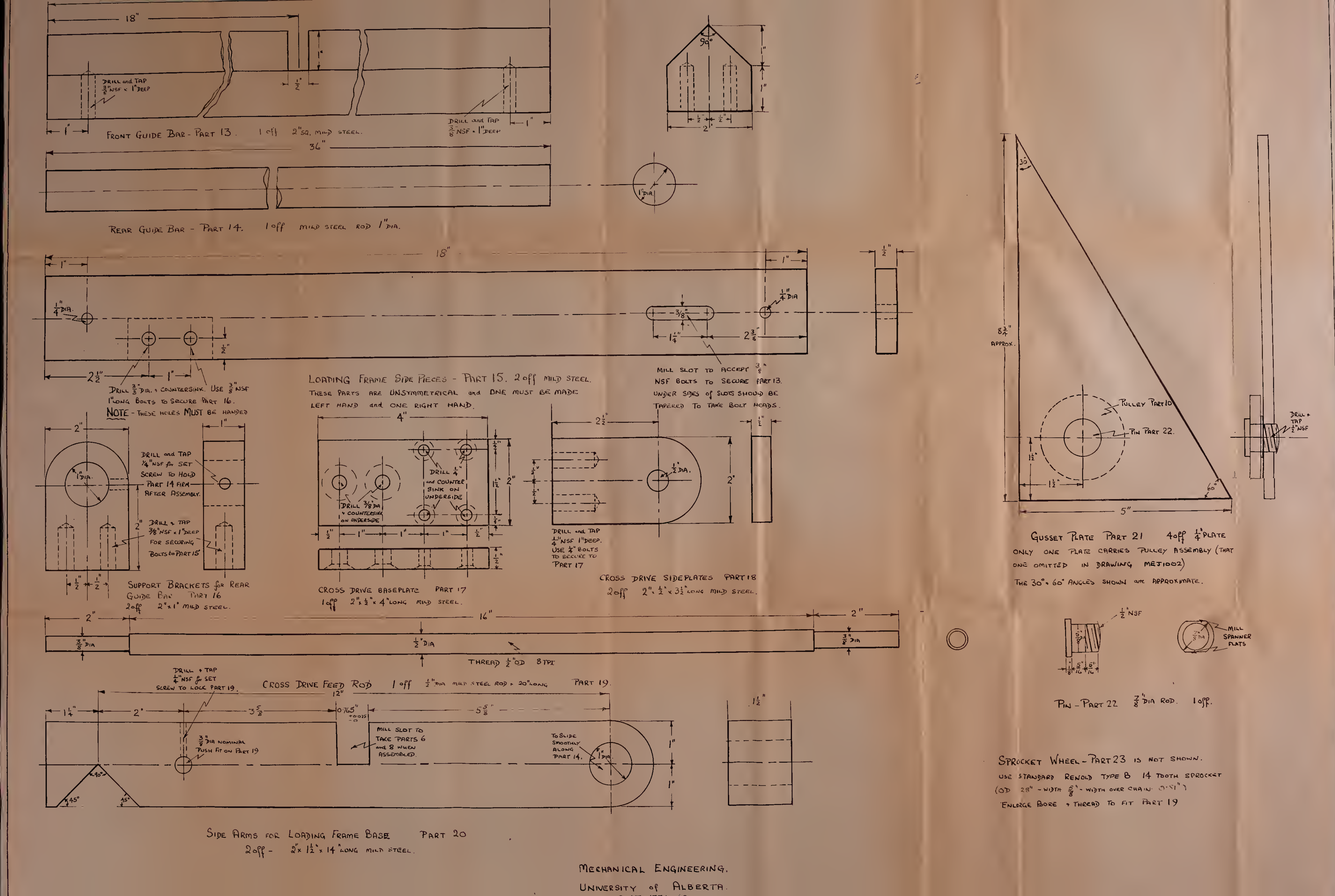

FRONT GUIDE BAR - PART 13. 1 off 2" SQ. MILD STEEL.
DRILL and TAP 3/8" NSF × 1" DEEP
REAR GUIDE BAR - PART 14. 1 off MILD STEEL ROD 1" DIA.
LOADING FRAME SIDE PIECES - PART 15. 2 off MILD STEEL.
THESE PARTS ARE UNSYMMETRICAL and ONE MUST BE MADE LEFT HAND and ONE RIGHT HAND.
DRILL 3/8" DIA. & COUNTERSINK. USE 3/8" NSF 1" LONG BOLTS TO SECURE PART 16.
NOTE - THESE HOLES MUST BE HANDED
MILL SLOT TO ACCEPT 3/8" NSF BOLTS TO SECURE PART 13.
UNDER SIDES of SLOTS SHOULD BE TAPERED TO TAKE BOLT HEADS.
DRILL and TAP 1/4" NSF for SET SCREW TO HOLD PART 14 FIRM AFTER ASSEMBLY.
DRILL & TAP 3/8" NSF × 1" DEEP FOR SECURING BOLTS to PART 15
SUPPORT BRACKETS for REAR GUIDE BAR PART 16
2 off 2" × 1" MILD STEEL.
DRILL 1/4" and COUNTER SINK ON UNDERSIDE
DRILL 3/8" DIA & COUNTERSINK ON UNDERSIDE
CROSS DRIVE BASEPLATE PART 17
1 off 2" × 1/2" × 4" LONG MILD STEEL.
DRILL and TAP 1/4" NSF 1" DEEP. USE 1/4" BOLTS TO SECURE TO PART 17
CROSS DRIVE SIDEPLATES PART 18
2 off 2" × 1/2" × 3 1/2" LONG MILD STEEL.
THREAD 1/2" OD 8 TPI
CROSS DRIVE FEED ROD 1 off 1/2" DIA MILD STEEL ROD × 20" LONG PART 19.
DRILL & TAP 1/4" NSF for SET SCREW TO LOCK PART 19.
3/8" DIA NOMINAL PUSH FIT ON PART 19
MILL SLOT TO TAKE PARTS 6 and 8 WHEN ASSEMBLED.
TO SLIDE SMOOTHLY ALONG PART 14.
SIDE ARMS FOR LOADING FRAME BASE PART 20
2 off - 2" × 1 1/2" × 14" LONG MILD STEEL.
PULLEY PART 10
PIN PART 22.
DRILL & TAP 1/2" NSF
8 3/4" APPROX.
GUSSET PLATE PART 21 4 off 1/4" PLATE
ONLY ONE PLATE CARRIES PULLEY ASSEMBLY (THAT ONE OMITTED IN DRAWING MEJ1002)
THE 30° & 60° ANGLES SHOWN ARE APPROXIMATE.
1/2" NSF
MILL SPANNER FLATS
PIN - PART 22 7/8" DIA ROD. 1 off.
SPROCKET WHEEL - PART 23 IS NOT SHOWN.
USE STANDARD RENOLD TYPE B 14 TOOTH SPROCKET
ENLARGE BORE & THREAD TO FIT PART 19
MECHANICAL ENGINEERING.
UNIVERSITY of ALBERTA.

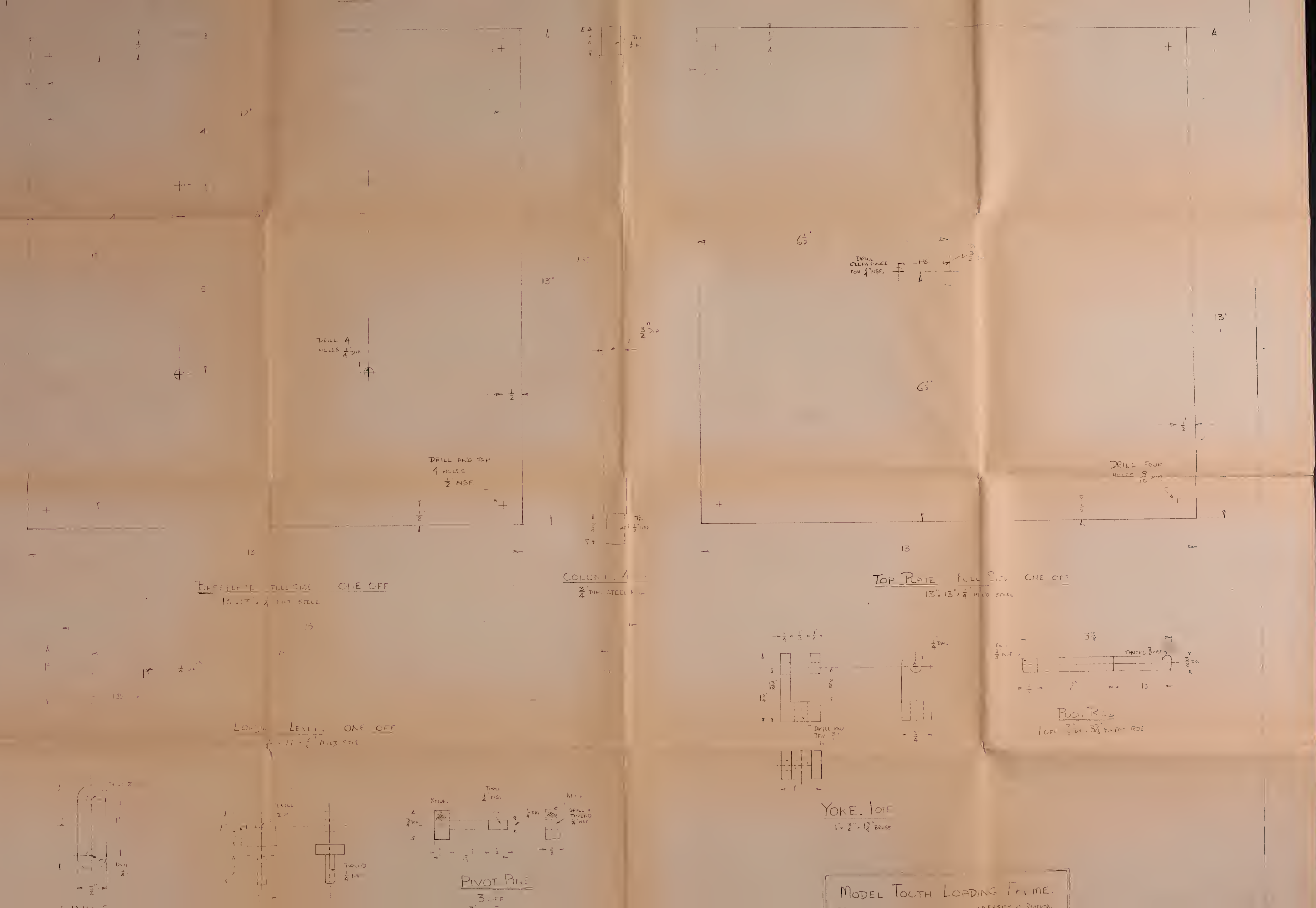

BASEPLATE FULL SIZE ONE OFF
13 x 17 x 1/4 MILD STEEL
DRILL 4 HOLES 1/4 DIA
DRILL AND TAP 4 HOLES 1/2 NSF
COLUMN A
3/4 DIA STEEL ROD
TOP PLATE FULL SIZE ONE OFF
13 x 13 x 1/4 MILD STEEL
DRILL CLEARANCE FOR 1/4 NSF
DRILL FOUR HOLES 9/16 DIA
LOWER LEVEL ONE OFF
YOKE. 1 OFF
PUSH ROD
PIVOT PINS
3 OFF
MODEL TOOTH LOADING FRAME.


2679


6L9D

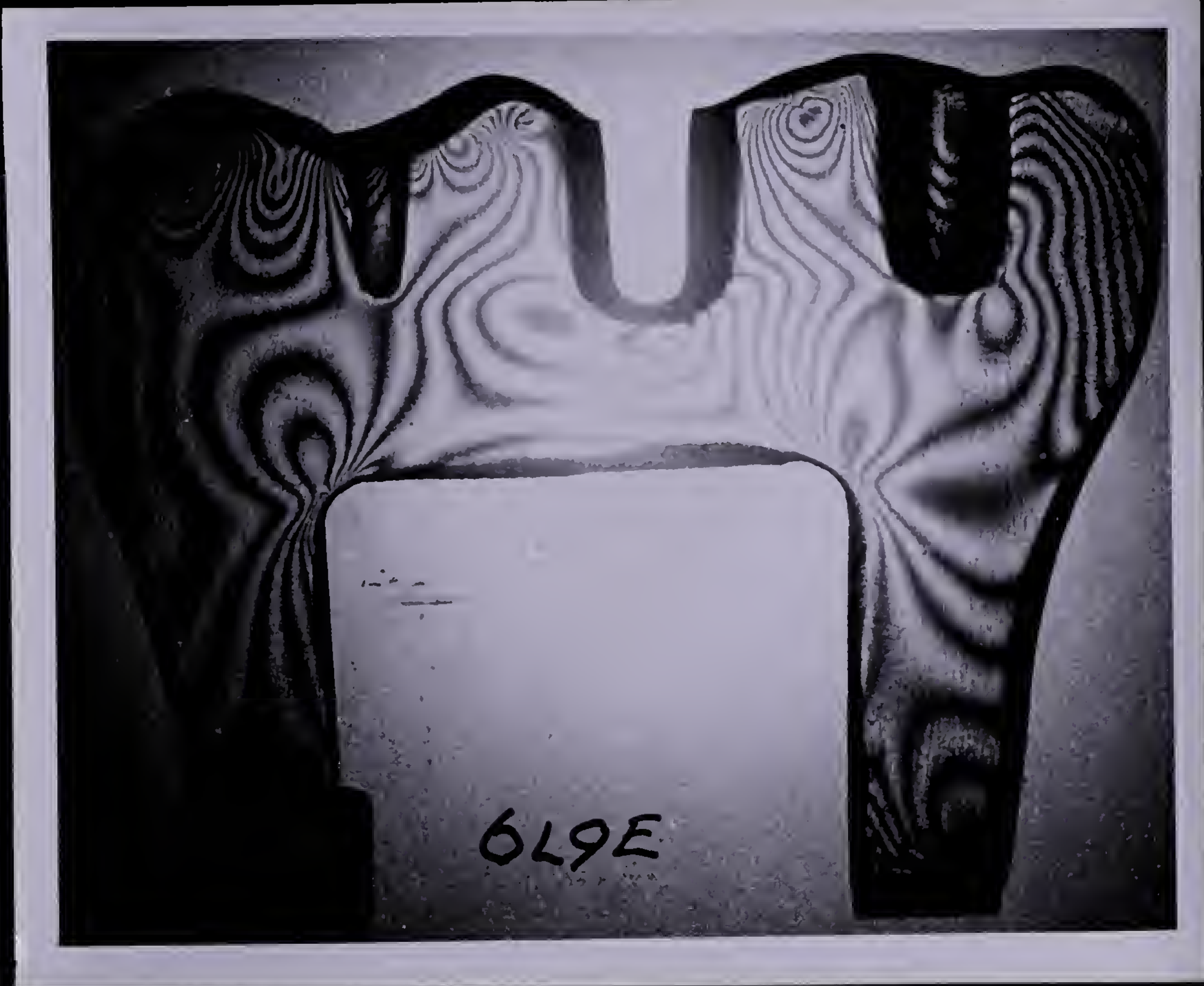


6L9F


H679


1679


GL13


6L13C


6L13D


6L13G


6L13H


6L13I


6


6413

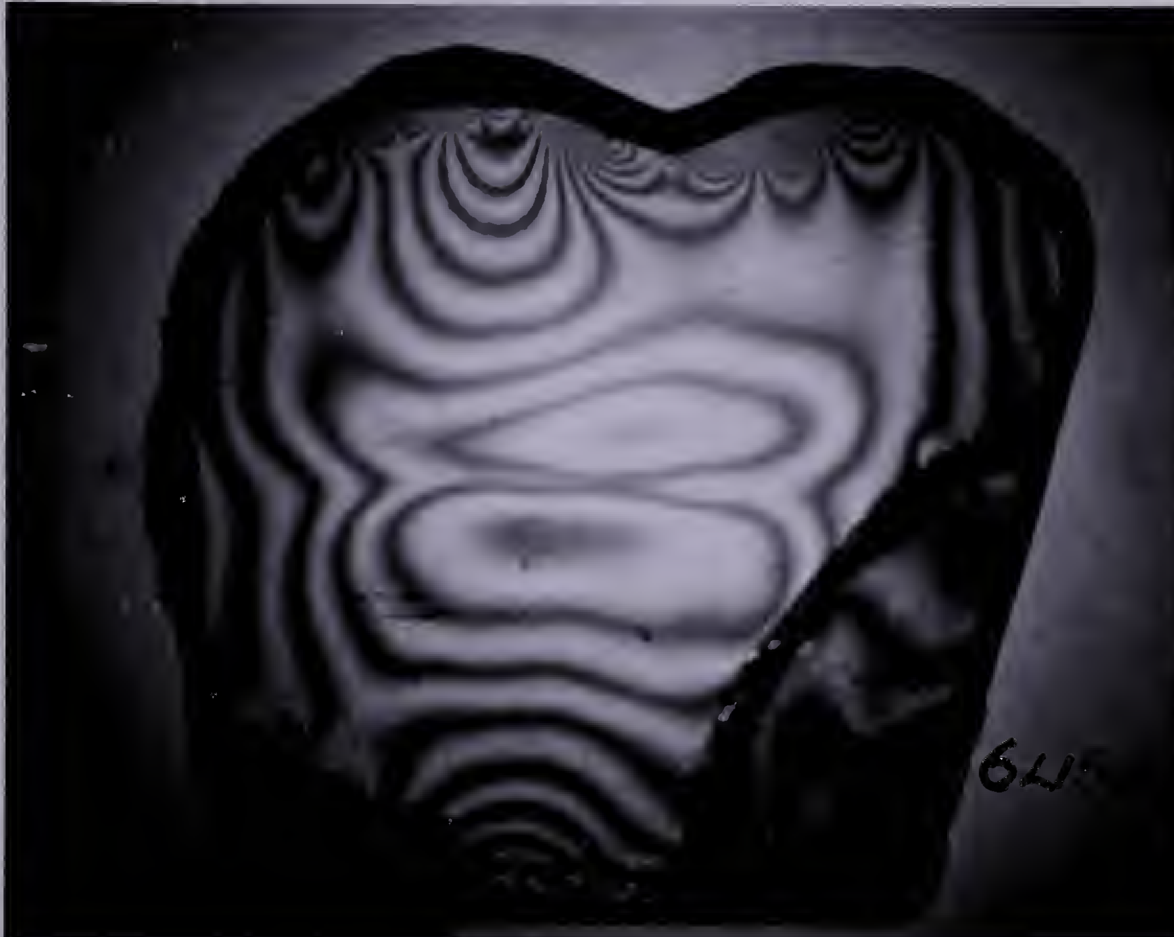


6L15C


6L15D


6LISE


6L15F


6L15G


6L15H


6L15I


6L15J